ASSESSMENT OF COMMERCIAL IMAGE PROCESSING SOFTWARE PROGRAMS FOR UNMANNED AUTONOMOUS VEHICLE IMAGERY

By

HECTOR YAMIL RODRIGUEZ ASILIS

A THESIS PRESENTED TO THE GRADUATE SCHOOL
OF THE UNIVERSITY OF FLORIDA IN PARTIAL FULFILLMENT
OF THE REQUIREMENTS FOR THE DEGREE OF
MASTER IN SCIENCE

UNIVERSITY OF FLORIDA

2012

To Abuela Ticha

ACKNOWLEDGMENTS

To my Dad and Mom, for supporting me in every decision I have made from the moment I was born, all the way through school and later my undergraduate studies, and also in the graduate studies I am completing now.

To my girlfriend Olga and my sister Yamilé, the two women of my life, they understand me in the good and the hard times.

To all the wonderful people I met in Gainesville, which every one of them have become family, they have been by my side in the great times and in the bad times in my journey through this town, with my beloved ones more than a thousand miles away, I will miss all of you, Ronald, Nico, Rodolfo, Gonzalo, Leonardo, Oscar, Pedro, Christobal, Robert, Kurtis, Luis, Julio, Kimmel, Bora, Alessio, Felix, Ivelisse, Angelica, Gisselle, Sonia, Rocio, Silvia, Sofia, Martha, Angie, Luisa.

To my Advisor Dr. Scot Smith, for being my support during this wonderful journey in the world of the Geomatics, in a totally new country for me.

To the University of Florida Unmanned Aerial Systems Research Group (UFUASRG) and the U.S. Army Corps of Engineers for giving me the opportunity to work with them in the post-processing and for trusting me, Matt Burgess, Bon Dewitt, Peter Ifju, Frank Percival, , Scot Smith, Damon Wolfe, John Perry, Tyler Ward and others.

TABLE OF CONTENTS

page

LIST OF TABLES

LIST OF FIGURES

LIST OF ABBREVIATIONS

2D	TWO DIMENSIONAL
3D	THREE DIMENSIONAL
AP	AERIAL PHOTOGRAMMETRY
AAT	AUTOMATIC AERIAL TRIANGULATION
ATP	AUTOMATIC TIE POINT
CE	CIVIL ENGINEERING
CMD	COMMAND PROMPT
DEM	DIGITAL ELEVATION MODEL
DGRS	DIRECTLY GEOREFERENCED REMOTE SENSING
DSM	DIGITAL SURFACE MODEL
DTM	DIGITAL TERRAIN MODEL
EM	ENSOMOSAIC
EOP	EXTERIOR ORIENTATION PARAMETER
EXIF	EXCHANGEABLE IMAGE FILE FORMAT
FAA	FEDERAL AVIATION ADMINISTRATION
FGDL	FLORIDA GEOGRAPHICAL DATA LIBRARIES
FWMD	FLORIDA WATER MANAGEMENT DISTRICTS
FWS	FLORIDA FISH AND WILDLIFE SERVICE
GCP	GROUND CONTROL POINTS
GNSS	GLOBAL NAVIGATION SATELLITE SYSTEM
GPS	GLOBAL POSITIONING SYSTEM
GSD	GROUND SAMPLE DISTANCE
IMU	INERTIAL MEASUREMENT UNIT
INS	INERTIAL NAVIGATION SYSTEMS

IOP	Interior Orientation Parameters
ISO	International Organization for Standardization
KML	Keyhole Markup Language
KPO	Kappa Phi Omega
LPS	Leica Photogrammetry Suite
NGS	National Geodetic Survey
OTF	On The Fly
RMSE	Root Mean Square Error
RPY	Roll Pitch Yaw
RTK	Real Time Kinematic
SLR	Single Lens Reflex
SUAS	Small Unmanned Aerial Systems
SUAV	Small Unmanned Autonomous Vehicle
UAS	Unmanned Aerial System
UAV	Unmanned Autonomous Vehicle
UAVP	UAV Photogrammetry
UF	University of Florida
UFUASRG	University of Florida Unmanned Aerial Systems Research Group
USACE	United States Army Corps of Engineers
USGS	United States Geological Survey
UTC	Coordinated Universal Time
UTM	Universal Transverse Mercator
VTOL	Vertical Take-Off and Landing
WGS84	World Geodetic System 1984

Abstract of Thesis Presented to the Graduate School
of the University of Florida in Partial Fulfillment of the
Requirements for the Degree of Master of Science

ASSESSMENT OF COMMERCIAL IMAGE PROCESSING SOFTWARE PROGRAMS FOR UNMANNED AUTONOMOUS VEHICLE IMAGERY

By

Héctor Yamil Rodríguez Asilis

December 2012

Chair: Scot Smith
Major: Forest Resources and Conservation

An Unmanned Aircraft System (UAS) was used to acquire digital images and produce geo-rectified mosaics, providing data and images to support ecosystem restoration, invasive species control monitoring, levee safety monitoring, and emergency natural disaster response.

A weakness of the system is extensive data post-processing requirement. The large volume of data collected on typical missions makes automated processing attractive. One of the primary advantages for the use of this system was the speed and low cost with which it can be deployed, but delays introduced by current data processing workflows that require extensive manual effort reduce this capability.

The research in this thesis was to investigate, (1) evaluate and identify appropriate software to streamline the pre/post-processing for delivering geospatial data in support of the topics described above, (2)enhance the processing workflow which includes camera geometric and radiometric calibration, (3)radiometric data processing, geospatial data pre-processing, (4)sparse tie point generation, (5)photogrammetric adjustment, (6)tie point densification, (7)terrain generation, (8)seam line generation, (9)radiometric correction, (10)mosaic generation and (11)establish an appropriate

amount of side slap coverage and overlap area for the proper flight appropriate needed according to the software being evaluated.

Three software programs were evaluated: (1) Erdas LPS, (2) 2d3 Altimap and (3) EnsoMosaic: The expected results were that: (a) the 2d3 Altimap would be the fastest and require less manual input, but that it would produce a less accurate solution, (b) EnsoMosaic would be the most accurate of the three and require less manual input than Erdas LPS, but be relatively slow.

CHAPTER 1
INTRODUCTION

Unmanned Aerial Systems Research Project

The Unmanned Aerial Systems Research Group, Florida Cooperative Fish and Wildlife Research Unit's multidisciplinary UAS research program (UFUASRG) with the University of Florida Department of Aerospace and Mechanical Engineering's Micro Air Vehicles Laboratory, the UF School of Forest Resources and Conservation's Geomatics Program, and the U.S. Army Corps of Engineers (USACE) is actively working towards the development of a small UAS for aerial imagery collection for natural resource assessments and monitoring applications.

The initial motivation to explore UAS applications for natural resource applications was to save lives. Due to challenging terrain and low altitudes characteristic of aerial surveys, light aircraft crashes are the leading cause of workplace mortality among wildlife biologists (Watts *et al.*, 2010). This research demonstrates the benefits of UAS such as rapid development, amphibious operation, high spatial accuracy, high resolution imagery and completely autonomous flight operation.

Development of the UASs was focused on for specific applications to the Army Corps of Engineers (USACE), such as monitoring invasive aquatic plant species, and the Florida Fish and Wildlife Service (FWS), like wildlife population research, these among other application has been able to be performed with the developments of the systems.

In 2011 a project (“Assessment of UAS Image and Navigation Processing Software and Nominal Sensor Enhancements”) for the UFUASRG was funded. Where the UF UAS would be used to take digital aerial images and produce geo-rectified

.mosaics, it would give data and images to the USACE to support ecosystem restoration, invasive species control monitoring, levee safety and emergency natural disaster response.

The Federal Aviation Administration (FAA) gave permission for certification of the UF UAS airframe to fly in portions of the Everglades. The platform had more than 2 years of deployment and testing and the large volume of data collected on typical missions makes automated processing attractive. The current data processing approach requires extensive manual effort while investigations have shown that there are ways to improve methodologies without affecting the aircraft used.

The objectives of the project include (1) assessment of appropriate software to modernize the pre/post-processing, (2) a workflow that will include camera geometric and radiometric calibration, (3) radiometric data processing, (4) geospatial data processing, (5) sparse tie point generation, (6) photogrammetric adjustment, (7) tie point densification,(8) terrain generation, (9) seam line generation, (10) radiometric correction and (11) mosaic generation.

A second objective of this project was integration of Dual Frequency RTK GPS receivers that permitted higher accuracy direct geo-referencing techniques which will facilitate more efficient post-mission image processing workflows. In addition using a high-end camera with an electronic/communication interface which allows for better efficiency in collecting data and permits to change to new cameras without reconfiguring the payload control software.

Buyuksalih and Li utilized a similar approach that the one used for the project of this thesis, but for different and older software packages, that are also not off-the-shelf commercial software (Buyuksalih and Li, 2003)

Unmanned Aerial Systems

UAS are remotely piloted light aircraft that can carry sensors in support of remote sensing applications. Although the basic concept of designing small remotely piloted aircraft has been known for decades, recent advances in miniaturization, communications, strength of lightweight materials and power supplies have permitted significant advances in UAS design.

The UF UAS was powered either by an electronic engine. It has a wingspan of approximately 2 meters and flight duration of approximately 1 hour.

Navigation can be controlled by remote radio signals, usually given by an operator who can directly observe the UAS in flight or use remote television images to view the terrain observed by the UAS. They can also be semi-autonomous, autonomous, or have a combination of these capabilities.

The term UAV is commonly used in computer science, robotics and artificial intelligence, as well as photogrammetry and remote sensing communities. Other synonyms could be, Remotely Piloted Vehicle (RPV), Remotely Operated Aircraft (ROA), Remotely Piloted Aircraft (RPA), Unmanned Vehicle System (UVS) and Unmanned Aerial System (UAS) can also be found frequently in publications. The FAA has adopted the latter (UAS), which was originally introduced by the U.S. Navy. (Eisenbeiss, 2009) Common understanding is that technology UAS represents the entire system, including the Unmanned Aircraft (UA) and the Ground Control Station (GCS).

UAS can carry cameras a variety of sensors depending on the application, and data can be recorded for retrieval after the UAV has landed, or it can be transmitted via telemetry to a ground receiver.

UAS remote sensing sensors include electromagnetic spectrum sensors, gamma ray sensors, biological sensors, and chemical sensors. A UASs electromagnetic sensors typically include the visual spectrum, the near infrared spectrum s as well as microwave. Biological sensors are capable of detecting the airborne presence of various microorganisms and other biological factors.

Limitations of UAVs

Current limitations include (1) initial acquisition costs for the UAS, (2) crew training requirements, (3) limited availability of high quality and lightweight sensors, and (4) FAA regulations for operating a UAS in the national airspace.

UAVs limit the sensor payload in weight and dimensions so that often low weight sensors like small or medium format amateur cameras are sometimes used. UAS have to acquire higher number of images so they can obtain the same image coverage and comparable image resolution. These payload limitations require the use of low weight navigation units which yield less accurate results for the orientation of the sensors. Also, because of the nature of these artifacts, they can not achieve high flying heights.

Existing commercial software packages applied for photogrammetric data processing are rarely set up to support UAS images therefore there are no standardized workflows and sensor models.

Photogrammetry

> Photogrammetry is the art, science and technology of obtaining reliable information about physical objects and the environment through the process of recording, measuring and interpreting photographic images and patterns

of electromagnetic radiant imagery and other phenomena (American Society of Photogrammetry, 1980).

Aerial Photogrammetry

Aerial or conventional photogrammetry utilizes large format imagery and ground coordinate information to effectively recreate the geometry of a portion of the earth in a virtual environment. In environment, reliable horizontal and vertical measurements can be made and compiled directly into a geospatial data file. To take accurate measurements from aerial photographic images, the following conditions have to meet: two or more overlapping stereoscopic images cover the object to be analyzed; accurate x, y, and z coordinates are known for at least three defined object points in the overlapping photographs; and a calibrated mapping or metric camera is used to take the photographs. The compilation of planimetric features and topographic information from the photographic sources is accomplished through the use of digital stereoscopic instruments. Digital photogrammetric workstations require specialized software and hardware for viewing a pair of stereo images. An experienced operator can link the images with the ground control to collect precise horizontal and vertical coordinates for a point, line, polygon, or surface. The photogrammetric workstation recreates the geometry of the field subject through a series of mathematical operations. These procedures require a high level of expertise and repetition to maintain the operator's skill. The softcopy instrument has analytical capabilities to a precisions level of under millimeters level. Thus, high-accuracy ground control coordinate positions are needed to fully exploit the analytical capabilities of these instruments.

UAS Photogrammetry

UAS photogrammetry describes a photogrammetric measurement platform, which operates remotely controlled, semi-autonomously, or autonomously, without a pilot sitting in the vehicle. The platform is equipped with a photogrammetric measurement system, including, but not limited to a small or medium size still video and/or video camera, thermal or infrared camera systems, airborne LiDAR system, or a combination of these. Current standard UASs allow the registration and tracking of the position and orientation of the implemented sensors in a local or global coordinate system. Therefore, UAS photogrammetry can be understood as a new photogrammetric measurement tool. UAS photogrammetry opens various new applications in the close range domain, combining aerial and close range photogrammetry, but also introduces near real time application and low cost alternatives to the classical manned aerial photogrammetry (Eissenbeiss, 2009).

Comparison

To compare the three forms of photogrammetry described earlier, one can start with the planning, which in AP it usually is semi-autonomous, in UAS it is automatic and manual; the data acquisition could be assisted or manual for AP, and autonomous, assisted or manual for UAS. For AP the project area size is several square kilometers, and square meters up to square kilometers in UAS. Resolution and GSD wise, UAS having within millimeters and meters resolution and centimeters to meters for. About distance to object and sensor to object orientation AP being 100 meters to 10 kilometers and meters to kilometers from object in UAS Photogrammetry, both normal and oblique case are used for the two types.

The AP has an accuracy of initial values of centimeters to decimeters, its normal block size is between 10 to 1000 images, and UAS has a centimeter to 10 meter accuracy and 100 to 1000 images per block.

Automatic Tie-point Extraction

One of the most complex and time consuming processes in photogrammetric workflow is the extraction of corresponding points in two or several images. Tie point extraction is the first step of aerial triangulation meant for computing the positions of the projection center and orientation of each image. The automation of the tie points extraction is challenging, especially when nonstandard approaches such as cameras mounted, usually digital and non-metric, on UASs or oblique imagery are used (Shragai *et al.*, 2012) Another reason for the increase in interest is the larger number of images produced for photogrammetric studies, in part by the use of the before mentioned digital cameras and strong overlaps (notably interstrips) on the other hand, generate images in greater number than in the past.

A tie point is a point whose ground coordinates are not known, but is visually recognizable in the overlap area between two or more images. The tie points can also be measured manually. Tie points should be defined in all images. They should show good contrast in two directions, such as the corner of a building or a road intersection. Tie points should also be distributed over the area of the block (Erdas, 2011).

Automatic tie point extraction is one of the major focal points of research and development in photogrammetry in recent history. The automation of aerial imagery photogrammetric processing aims at the production of tie points and their use in two domains: the aerotriangulation itself and the automatic realization of index maps, which is a preliminary step in any triangulation process (Shragai, 2012).

This automatic tie point extraction is in special interest for this research, first because without the use of GCPs, we have to rely completely on interior and exterior orientation parameters to measure tie points and consequently match images together on the mosaics, and second because it is a good measure of software productivity, according to speed and accuracy of the entire processing, where this part may dictate the main difference between programs.

There are different aspects of the scene that can actually impact the point extraction and these are variation of aspect of objects, where the can vary depending of the position of the object in relation to the sensor. Forest, shades and textures, these three together create problems in image analysis. Trees cause problems of precision of pointing; shades move between two image acquisitions, notably between two strips, even though they are easy to delineate they are not valid in a photogrammetric point of view. Textures can lead to problems of identification. It is easy to confuse two very similar details in zones with repetitive motives. Relief, this provokes notable changes of scale and variations of discrepancy. When looking for homologous points, the space of research is generally larger (Ghosh, 2005).

For the study of tie point extraction one have to take into account 3 different factors: reliability, precision and minimum number of tie points. Most of the algorithm and methods use least square adjustment technique which is sensitive to aberrant values. Therefore one of the objectives is to find a method that provide points that are exempt from mistakes. Second, at the end of the extraction and aerotriangulation, one has to take into account a good model that can correct the errors in point extraction. Finally is the number of tie points needed by the software in order to be able to later run

the bundle block adjustment; Erdas LPS needs a minimum of 6 points for every image, while EnsoMOSAIC needs 6 points in each of the four quadrants in the image, and at least 4 points per image pair.

2d3 Altimap detects the feature points, then analyzes the image set connectivity determining feature point correspondences guided by GPS data. The image matching strategies incorporated in Erdas LPS for tie point generation include the coarse to fine matching, feature based matching with geometrical and topological constraints, a simplified method from structural matching algorithm (e.g., Wang, 1998), and least square matching for high accuracy of tie points.

Aerial Triangulation Techniques

Aerotriangulation is the term most frequently applied to the process of determining the X, Y and Z ground coordinates of individual points based on photo coordinate measurements. Today, the accuracy of the ground coordinates using these techniques are within decimeters depending on the payload used (Krystek *et al.*, 1996).

Aerotriangulation is used for many purposes in photogrammetry and for most of the applications; the minimum number of control points is 3. For large mapping projects, the number of control points increase. The use of Real-Time Kinematic (RTK) GPS in the aircraft to provide coordinates of the camera at the instant each photograph is exposed. This technique has eliminated the need for ground control (Wolf and Dewitt, 2000).

2d3 Altimap uses a two-dimensional (2D) block adjustment algorithm, then ortho-rectifies and geo-register the mosaics applying auto level correction and color balancing.

Erdas LPS uses Bundle Block Adjustment techniques that uses itself collinearity condition as the basis for formulating the relationship between image space and ground space. The collinearity equations are solved using least-squares adjustment to (1) estimate the values of exterior orientation, (2) estimate coordinates of tie points, (3) estimate interior orientation and (4) minimize and distribute data error through the network of observations. LPS also allows the interior orientation parameters to be analytically calibrated with its self-calibrating bundle block adjustment. LPS offers robust error detection methods within the triangulation process to eliminate gross errors.

Bundle Block Adjustment

Almost all analytical aerotriangulation methods consist of writing condition equations that express the unknown elements of exterior orientation of each photo in terms of camera constants, measured photo coordinates, and ground coordinates. These equations are solved to determine the unknown orientation parameters and subsequently coordinates of pass points are calculated.

The bundle block adjustment allows the orientation of a block of an unlimited number of photographs using only three GCPs. This requires that relative orientation of the individual images within the block first established by additional tie points/image points with unknown ground coordinates which appear on two or more images and serve as connections between them, as shown on Figure 1-1. The tie points can be identified manually or with automatic matching procedures. The term bundle refers to the bundle of light rays passing from the image points through the perspective center to the object points.

The exterior orientation parameters has become important in bundle adjustment with the use of airborne GPS control and Inertial Navigation Systems (INS) which have the capability of measuring the angular attitude of a photograph.

Use of GPS in Aerotriangulation

As mentioned before, the aim of aerotriangulation is to reduce as much as possible the requirement of field measures, by processing simultaneously the geometry of several images. Aerotriangulation will adjust the measures of coordinates in the images of the homologous tie points, known ground control points, auxiliary measures recorded during the flight, or even satellite trajectography data.

Digital photogrammetry itself brought up the measure of tie points to be automated completely and the development of digital cameras, as they require more images to cover a the project area, led to the search for more efficient auxiliary measures in order to restrict again the ground measures. All these led to the implementation of highly accurate GPS control on aircraft for the use of aerotriangulation methods.

The precision needed on the GPS observation need to be at least as good as that of the points to localize on the ground. These precisions can vary between 5cm and 30cm, and with sometimes high speed of the planes, that means a good synchronization between camera and GPS receiver. It is necessary that the camera provides a signal perfectly synchronous with the opening of the shutter. Also, with GPS measures every second one has to interpolate the position of the camera at the time of the signal of synchronization.

The UFUASRG is working on the implementation of RTK GPS antennas on the aircraft. These RTK modes which measure the phase on the signal carrier. The initialization can be done with a time duration permitting the ambiguity resolution and

fixes it for the remainder of the mission, which the reliability is low, because due to the aircraft turning there is interruption of the signal, making it impossible to solve the ambiguity again on the flight. The other solution is to solve the ambiguities On-The-Fly (OTF), which for conventional photogrammetric flights can be a limitation because of a distance of at least 20 to 30 kilometers to the base, something that is not of a problem to UAVs. With the use of OTF solution, it is necessary to put a GPS station close to the zone of the photograph, which can be a implementation of a lot of time due to equipment set up, other solution is the use of a permanent GPS station close to the project.

Determination of the Attitude of the Aircraft

For a great measure of the attitude of the plane it is needed several GPS antennas with perfect synchronization and separated around the plane, for better precisions. At a higher cost but a better solution for the SUASs, due to lack of payload weight capability, is an Inertial System or Inertial Measurement Unit (IMU) integrated with the GPS unit, it can create a very accurate attitude measurement.

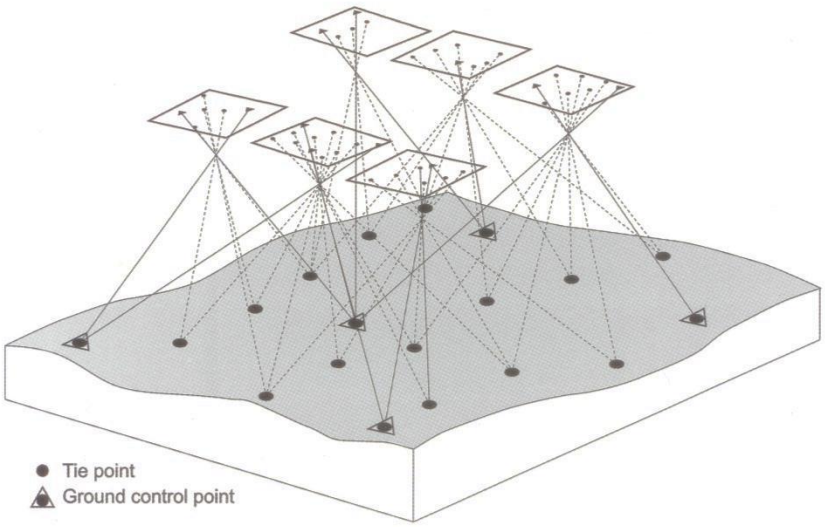

Figure 1-1. Principle of bundle-block adjustment. The relative orientation of the images in the block is established by both tie points and GCPs, the absolute orientation of the block within the ground coordinate system is realized using GCP coordinates. Source (Aber *et al.*, 2010).

CHAPTER 2
LITERATURE REVIEW

UAS Uses and Applications

The adoption of remote sensing using UAVs in archaeology is proposed by Eisenbeiss, (2009). The main purpose is to document archaeological sites, and to provide better resolution imagery. The accuracy requirements are not very high, although it has been shown that elevation accuracy using a helicopter UAV and a consumer digital camera yields elevation models that are comparable to ground laser scanner measurements.

Vegetation monitoring was successfully done using UASs. A Hale UAS, Pathfinder Plus was used to demonstrate this on a coffee plantation in Hawaii (Herwitz *et al.*, 2004), similar to others being use to study rangelands and has been considered to be an integral part of farm equipment (Rango, 2006).

Rapid response imaging using UASs has received a lot of attention as well. This has been demonstrated for road accident simulation (e.g., Haarbrink *et al.*, 2006) and also for forest fire monitoring (e.g., Réstas, 2006).

Qingyuan *et al.*, (2011) proposed a new UAS image mosaicking method which uses the homogenous points extracted from the imaging stitching. The fast mosaicking of UAS images contemplates an alternative to deal with fast mapping applications, such as disaster monitoring, human rescue (Qingyuan *et al.*, 2011)

The UFUASRG has used small UASs for restoration monitoring, wildlife surveys (bird detection and counting, manatee surveys, bison survey) , habitat assessments, forestry stand analysis, vegetation surveys (imagery can be used to measure area of

wetlands, vegetation coverage, habitat type, health of stands, restoration progress), storm damage assessments (Watts,*et al.*, 2010)

Other applications of UASs are power line inspections and surveying, where power lines and power corridors are mapped; snow cover and snow depth; ocean color where high resolution hyper spectral measurements enable measurements of chlorophyll and primary production in the ocean, Digital Elevation Models (DEM), mapping, atmospheric and meteorological measurement, environmental monitoring, like oil spills, flooding and algae blooms (Norut, 2012)

UAV-based photogrammetry has been used for accurate 3D mapping in mine areas. The workflow included ground control network design, image acquisition, 3D mapping and information extraction (Liu *et al.*, 2012).

The use of airborne differential GPS, with an accuracy of 2 to 4 cms, had been compared to the accuracy of using GCPs in UAVS photogrammetry, with similar values for both techniques, between 10 and 15 cm (Turner *et al.*, 2012).

Advances in Automatic Tie Point Extraction and Aerial Triangulation

Photogrammetric aspect, signal based matching or area-based matching, is a method that determines the correspondence between two image areas according to similarity of grey level values, cross relation and least square techniques are known methods for this kind of matching, the counterpart to this methods is the necessary to use perfectly oriented images with not much rotations (Erdas, 2010).

Area-based matching is also called signal based matching, which determines the correspondence between two image areas according to the similarity of their gray level values. Least squares correlation techniques are a well-known methods for area-based

matching. Least square correlation uses the least squares estimation to derive parameters that best fit a search window to a reference window. This technique has been investigated thoroughly in photogrammetry (Ackermanm, 1983; Grun *et al.*, 1988; Helava, 1988).

Kenned and Cohen, (2003) contemplated that correlation-based matching approach has great potential for use in general satellite remote sensing, citing that the grid of tie-point pairs produced by the this technique is regular, it is optimal for capturing the geometric relationships of images, moreover, the technique is repeatable, ensuring that image libraries built up over time have consistent geometric properties. It is relatively robust to simple distortions and inaccuracies. (Kennedy and Cohen, 2003)

Feature-based matching or signal aspect matching, it determines the correspondence between to image features, the feature points calculated with this methods are commonly called interest points. One operator is the Forstner Operator (Forstner and Gulch, 1987). LPS uses this operator where the image features must initially be extracted, and later the attributes of the features are compared between the two images.

Another automatic tie point technique relation-based, also called structural matching (Vosselamn and Haala, 1992), is a very which uses image features and the relationship between the features although this approach is very time consuming.

Wang developed a structural matching algorithm, where a fully automated matching of image features is realized without any a-priori information, even with images from amateur digital cameras was achieved (Wang, 1998)

Also, a new approach using linear features has being evaluated, contemplating that a typical aerial scene contains more linear features than well-defined points, and that control information from an object is more reliable than individual points. (Schenk, 2006).

Tree search methods has been developed and assessed on the applications and implications that could have in digital photogrammetry problems like object location and recognition, stereo image matching, edge and line following and geometric reasoning (Vosselman, 1995).

A tie point matching algorithm using least squares image matching techniques for UAS using video imagery, therefore the resulting images are very close to each other, meaning very high overlaps between images. Instead of searching an entire image or a large portion of an image for a conjugate point, the search was reduced to a subset of the image based on the point's coordinates in the previous image (Wilkinson, 2007)

Evaluations on aerial triangulation methods had been done, including a comparison between different additional parameter models, and an assessment of human performance versus computational performances (Tang *et al.*, 1997).

Self-calibrating bundle block adjustment methods use additional parameters in the triangulation process to eliminate the systematic errors. Self-calibrating methods are studied in (Granshaw, 1980) and (Konecny, 1994).

A procedure for automatic absolute orientation using aerial photographs and a map, an automated system for exterior orientation which first involves automatic relative orientation. This method has potential for use where existing maps are available and where sufficient detail is present on the image and on the map to ensure a large number

of well distributed points which can be used for orientation (Morgado and Dowman, 1997).

Other approaches like the of high redundancy in the multispectral aerial sensor input images to generate a land use classification, a DEM and true ortho-images (Zebelin *et al.*, 2006).

Heipke, (1997) approached the automation of interior, relative and absolute orientation with a more primitive way, using scanning of non-digital images, stating that is a more reliable technique than GPS and INS technology of his time.

CHAPTER 3
METHODS

Study Area

A data set was collected utilizing the (UF UAS) payload integrated onboard the UAS in order to evaluate minimum overlap and side lap required to create mosaics with the three photogrammetry software programs assessed (2d3 Altimap, EnsoMOSAIC, LPS). A flight plan consisting of ten parallel flight lines equally spaced twenty meters apart was prepared at Archer Fields, Archer, Florida. Imagery was collected at a rate of one exposure every 2.5 seconds. Each flight line was approximately 800 meters in length and orientated in a north-south direction. The flight plan was executed in a back and forth pattern; flying south to north on line one and returning from north to south on line two. This pattern was repeated for the ten lines. Upon completing flight line ten, the flight plan was flown again; back and forth, in the opposing direction (flying south to north on line ten and returning from north to south on line nine). This pattern was repeated for the ten lines back again in order to minimize the effects of inconsistent overlap due to wind speed. This flight plan was able to create different scenarios of overlap and sidelap coverage, for assessment of the software in different conditions. In Figure 3-1, shows where the number of strips are shown with wind direction and geotags of images on capture.

The following procedures were utilized to vary the exposure interval for this investigation: (1) process all data along the planned flight path (all flight lines, both directions); (2) process only exposures collected in the upwind direction along the planned flight path (all flight lines, north to south direction only); (3) process only exposures collected in the downwind direction along the planned flight path (all flight

lines, south to north direction only); (4) process only exposures collected in the upwind direction along the first back and forth pass of the planned flight path, utilizing every other line (even numbered lines, north to south direction only); (5) process only exposures collected in the downwind direction along the second back and forth pass of the planned flight path, utilizing every other line (even numbered lines, south to north direction only); (6) process only exposures collected in the first back and forth pass of the planned flight path (all flight lines); (7) process only exposures collected in the second back and forth pass of the planned flight path (all flight lines); (8) process only exposures collected in the upwind direction along the second back and forth pass of the planned flight path, utilizing every other line (odd numbered lines, north to south direction only); (9) process only exposures collected in the downwind direction along the first back and forth pass of the planned flight path, utilizing every other line (odd numbered lines, south to north direction only). For every step of this process explained above, a block was created in order to run separately all datasets on the software to be assessed. Table 3-1 shows the specifications of separation and overlap for every block, and Table 3-2 shows the lines and directions used for every block. On Figure 3-5 is a map of all 9 block configurations.

Determination of Ground Elevation on Center of Images

In order to get the elevation on the ground, on the exact position of the center of the images on the moment of capture, a five-foot contour line layer was downloaded from the Florida Geographic Digital Library (FGDL). This layer was clipped to the boundary of City of Archer. The contour line shapefile was later converted into a raster surface within the study area using the cleaned flight lines and geotags of the images taken with the UAS, which in result is a DEM of the study area shown in See Figure 3-2.

Later, the DEM was interpolated to the spatial position in the projection of the geotags, resulting in a new shapefile were the previous geotags file were added a new feature called elevation.

Calculation of Overlap Percentages

An important element in photogrammetry, is overlap percentages, both in forward and side, this is to permit any links and tie between adjacent images. Assessment of the impact of different overlap percentages on mosaic processing was made. The forward separation between flights was inconsistent due to wind gusts along the flight line. This was one of the reasons to use this flight direction to only have the incidence of wind on one direction.

The dataset was in WGS 1984 coordinates. To calculate distance in meters between images, the coordinates where transformed to UTM Zone 17 North projection, and distance was calculated between consecutive images along the flight path using a distance matrix. This distances where averaged per block configuration. The ground distance of an image side can be calculated with Equation 3-1, where S=ground distance of image S´=sensor size in millimeters, H_g= flying height, f=focal length.

$$S = \frac{S' x\, H_g}{f} \tag{3-1}$$

Equation 3-1 was used to calculate the ground side of every image. And then calculating an approximate overlap percentages using Equation 3-2, where S_1=ground distance of Image, and S_2 = ground distance of adjacent image. These values were averaged for all the blocks.

$$p\% = \frac{\frac{S_1}{2} + distance - \frac{S_2}{2}}{S_1} \tag{3-2}$$

Tree and Cloud Coverage per Image

In order to estimate the impact of tree and cloud in photogrammetry processing, a manual survey was done to the entire dataset. A percentage of tree and cloud coverage was measured for every single image.

Workstation Specifications

The workstation used for this evaluation was an HP z800 Workstation, with an Intel Xeon W55880 @3.20 GHz 3.20 GHz Processor and a 48.0 GB Memory Ram, in a Windows Vista Professional 64-bit Operating System.

UF UAS Payload Output Data

Each flight automatically generates a folder labeled with the time and date. The folder contains two elements, the image files and a log file. The format of the image files is by default .jpg, although the image format is selectable. The log file is generated in real time and combines the information from all payload sensors but the images into a single ASCII file. The log is formatted with each line corresponding to a data or status packet, prefixed by a 3 letter code indicating the source of the packet. The log file is parsed and the packets processed to produce an output file, the geotags file, which provides the direct georeferencing parameters associated with each image. The parameters are calculated by interpolation of the navigation packets using a “Burredo” synchronization packets associated with the image exposure. The “Burredo” is synchronization device, manufactured by the UF team, designed for synchronization between a the Olympus E-420 and an INS/GPS. The “Burredo” allows for synchronization of a wide range of sensors with minor modifications to the signal conditioning circuitry to handle the voltage level. (Perry, 2009).

The geotag file is the one that was used for all the post-processing, it contains: Image name and folder path; longitude and latitude, in decimal degrees; ellipsoid height, in meters; and the image orientation (pitch, roll and yaw), in the form of omega, phi, kappa in degrees.

For the omega, phi and kappa values, we have to visualize XYZ coordinate system in the origin of the focal point (center of image), omega is a rotation about the photographic x-axis, phi is a rotation about the photographic y-axis and kappa is a rotation about the photographic z-axis as shown in Figure 3-3.

Non-Vegetated Area of Study

The forested area in Nortrth side of Archer Fields Area has dense vegetation, making impossible to process data on that zone with Erdas LPS, therefore a smaller non-vegetated area of study (270 meters long, 120 meters wide) was created for every block keeping the forward and side overlap percentage values, to be able to make a comparison between LPS and EnsoMOSAIC. The Area has (270m x 120m). The clipped area is shown in Figure 3-4.

Table 3-1. Block Configuration and Properties

Block Configuration	Images	Distance (m) Fwd	Std	Side	Overlap (%) Fwd	Side	Average (m) Ground	Height	X Grnd	Y Grnd
0	335	24.98	12.22	20	73.86%	72.07%	25.05	162.88	95.47	71.60
1	221	33.98	4.76	20	62.26%	72.03%	25.05	162.68	95.33	71.50
2	114	72.75	5.87	20	27.86%	72.14%	25.04	163.25	95.73	71.80
3	113	35.13	4.43	40	63.11%	43.92%	25.10	162.39	95.10	71.32
4	57	68.31	5.93	40	29.13%	44.63%	25.02	164.08	96.32	72.24
5	170	48.26	17.17	20	49.34%	71.96%	25.09	162.40	95.11	71.34
6	165	47.41	15.77	20	50.62%	72.17%	25.01	163.37	95.83	71.88
7	108	36.88	4.96	40	61.45%	44.20%	25.01	162.99	95.58	71.68
8	57	69.91	5.79	40	26.53%	43.95%	25.06	162.42	95.15	71.36

Table 3-2. Block Configuration Flight Lines and Directions

Block Configuration	Direction	Flight Path	Flight Lines Downwind (North)	Flight Lines Upwind (South)
0	All	Both	1, 2, 3, 4, ,5, 6, 7, 8, 9, and 10	1, 2, 3, 4, ,5, 6, 7, 8, 9, and 10
1	Upwind	Both	None	1, 2, 3, 4, ,5, 6, 7, 8, 9, and 10
2	Downwind	Both	None	1, 2, 3, 4, ,5, 6, 7, 8, 9, and 10
3	Upwind	First	None	2, 4, 6, 8 and 10
4	Downwind	Second	2, 4, 6, 8 and 10	None
5	All	First	1, 3, 5, 7 and 9	2, 4, 6, 8 and 10
6	All	Second	2, 4, 6, 8 and 10	1, 3, 5, 7 and 9
7	Upwind	Second	None	1, 3, 5, 7 and 9
8	Downwind	First	1, 3, 5, 7 and 9	None

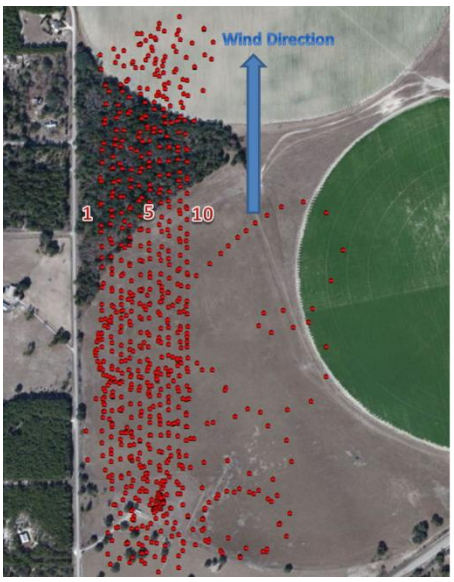

Figure 3-1. Map of flight mission. Including of the satellite imagery of AOS, wind direction, Strip numbers.

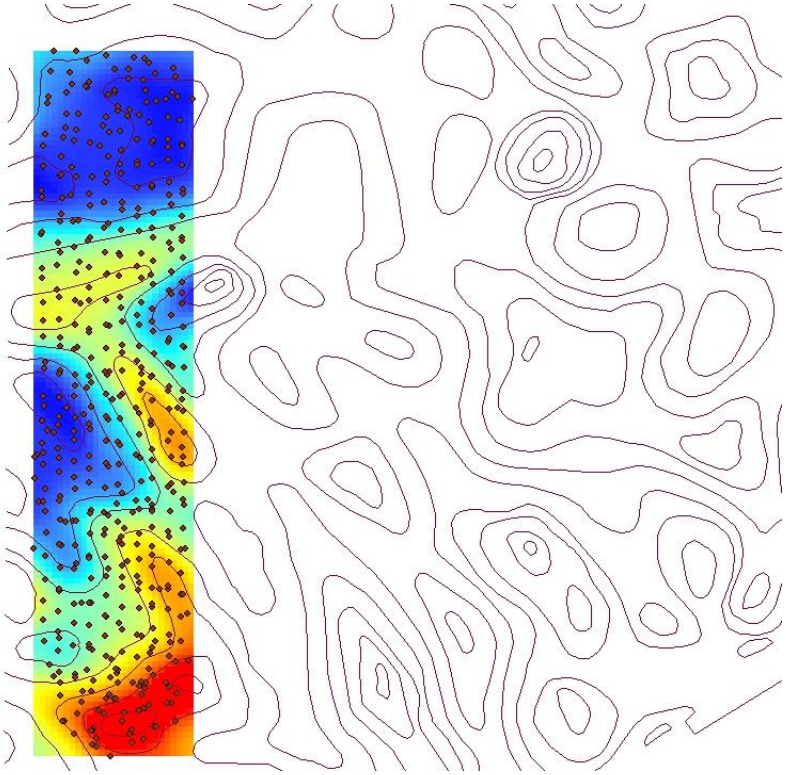

Figure 3-2. Contour Line Data, Flight Plan and Digital Elevation Model. A view of the Contour Line Shapefile downloaded from FGDL along the image captures and the Digital Elevation Model created using the ArcGIS 10 software.

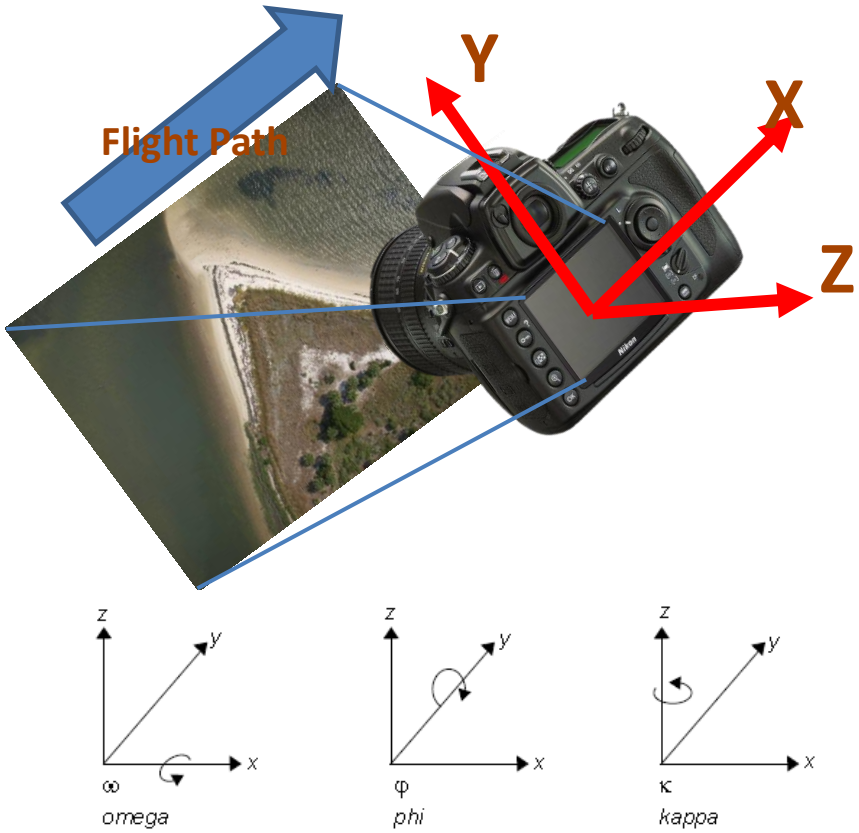

Figure 3-3. Image Exterior Orientation Parameters: Omega, Phi and Kappa.

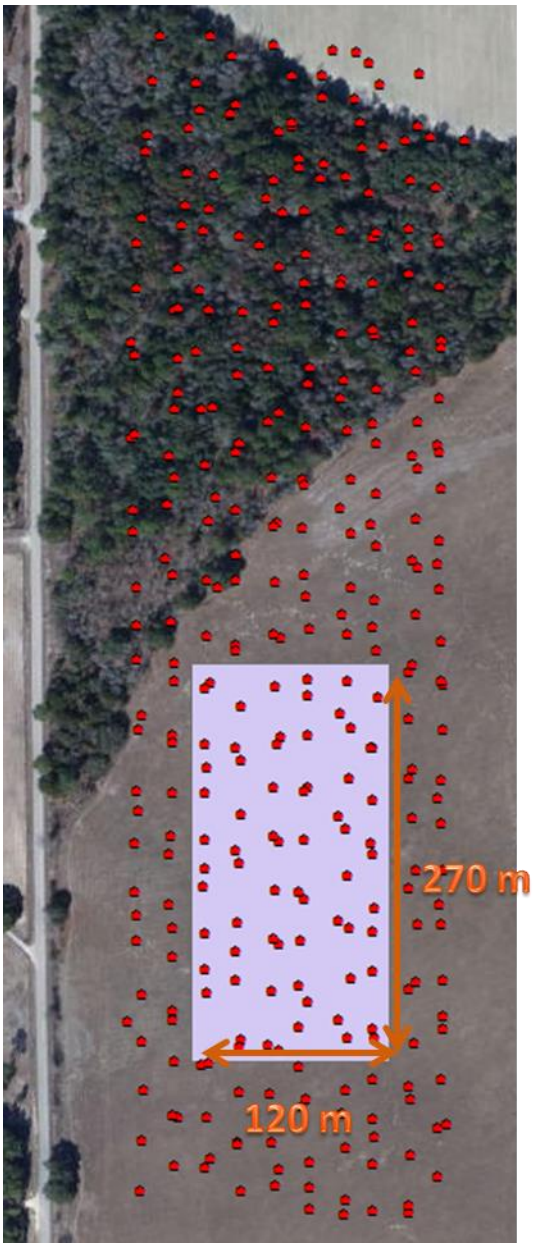

Figure 3-4. Non-vegetated area of study.

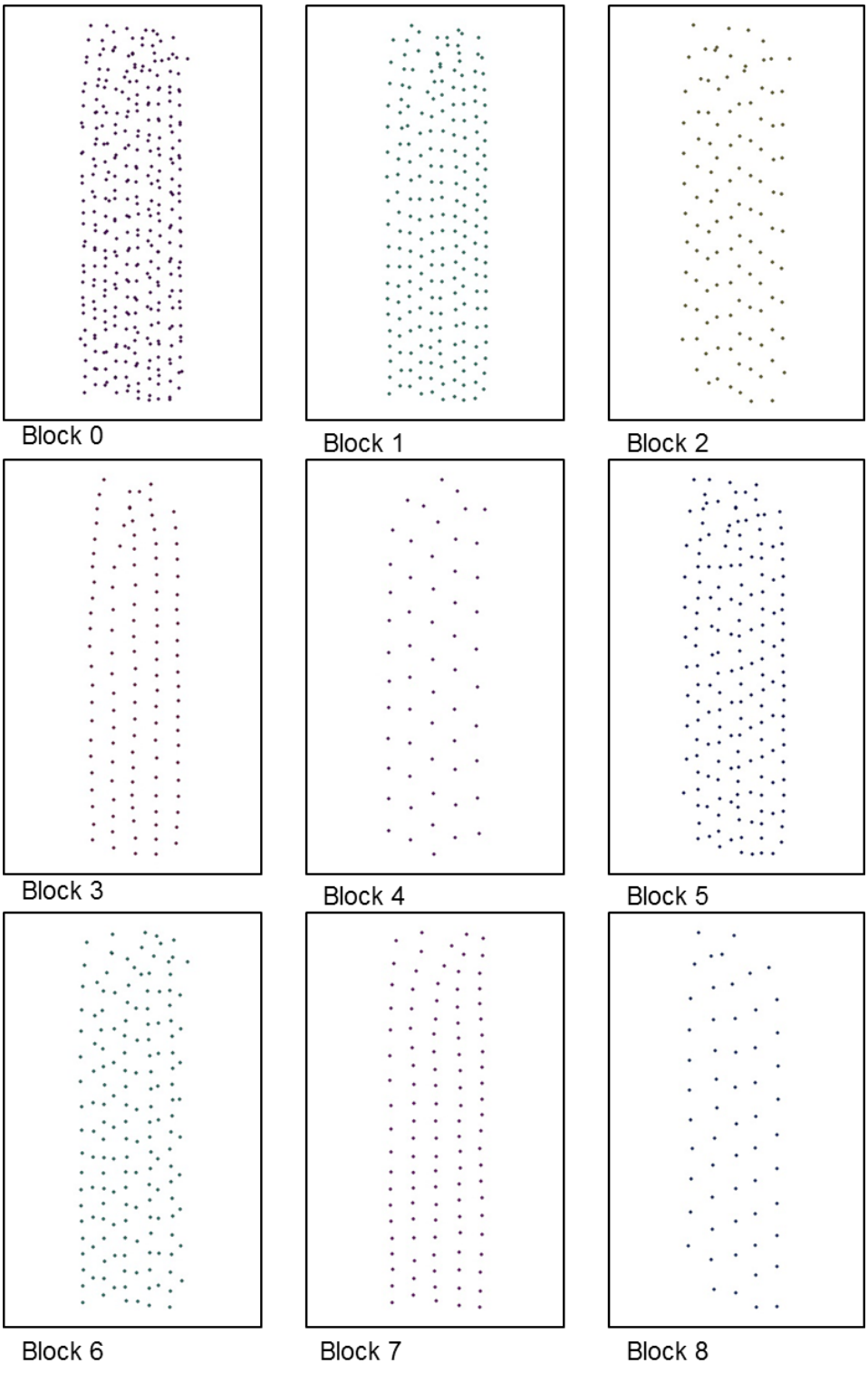

Figure 3-5. Block Configurations.

CHAPTER 4
RESULTS AND DISCUSSION

2d3 Altimap

2d3 Altimap is an inexpensive solution to solve mosaicking for low altitude flying aircrafts. This solution has the ability to correlate the images in “image space” by the images themselves alone. If there is EXIF header about the GPS position of the image, the software will geo-locate the resulting mosaic.

2d3 Altimap automatically compares features in each image with other images to determine their match in image space, a process called Wide Baseline Matching, making 2d3 Altimap great for processing even if no data is available from the imagery. If the image dataset provided by the user does not have enough overlap, 2d3 Altimap will create separate mosaics for cases where there is no overlap in the image sets.

Altimap will read JPG, BMP, PNG and GIF imagery files provided by the user, and NMEA, XML, EXIF and TXT data files. Altimap will output mosaics in JPG and PNG imagery files, and also KML, Tile Map Specification and XML creating an output mosaic that can be exported to Google Earth, KML File, and it can be viewed on the current location of the imagery, just like geolocated orthoimages.

The different capabilities of the Altimap software are mosaicking, which by using highly accurate image registration it will stitch together adjacent images, and use them to create a large mosaic. This capability can also be used with video recording in an aircraft; two-dimensional feature extraction, which is that the program will detect and identify hundreds and thousands of features in a scene and follow their motion throughout a sequence using a form of corner detection and also has the capacity to match and track shapes as they change in two dimensions with their relative orientation

to a moving camera. This can be helpful in the identification of fiducial style markers. The camera's tracking technology makes it possible to calculate the path of the originating camera in three dimensional space and describe the three dimensional position of two dimensional features within the source image sequence. For a stream of multiple still images, the structure from motion approach involves the automatic identification of hundreds and thousands of distinctive points that appear in areas of high contrast or high texture. Structure from motion enables the three dimensional movement of the camera to be inferred from the 2d motion observed in the image sequence. Visible in the image above is a red line indicating the inferred trajectory of the camera in 3d space and the camera view frusta for some of the frames.

2d3 Sensing

2d3 Sensing is a remote sensing company that specializes in computer vision softwares and solutions for imagery, metadata acquisition and processing. 2d3 started to adapt their technology for use in aerial imaging applications, developing products covering a wide range of real time and off line computer vision capabilities for processing of aerial motion imagery. Designed from the ground up for analyzing and processing motion imagery, these products won the company a lot of contracts with the military and commercial business for remote sensing and security.

2d3 acquired Sensing Systems which had developed and fielded a motion imagery software development media toolkit. 2d3 Sensing, the resulting combined entity, offers a complete spectrum of software technology for the management, enhancement, exploitation, and dissemination of imagery and metadata.

2d3 Data Preparation

The 2d3 Altimap works taking images with EXIF data written to them, with longitude, latitude and height information. The image that Altimap uses has to be at a specified directory, and the output data will also be located in this folder. The Altimap software is the easier of the three programs assessed to work with. The one with less steps is written in a CMD format script, and to facilitate the handling, a python script was written to do some of the preliminary data preparation on one script.

Image Cleaning

In order to use the correct image data to be processed with 2d3 Altimap, the first step is to clean and create blocks using the geotags file to create feature points in a GIS software like ArcGIS or QGIS. To start the filtering process, we can start after the first hundred or so images usually, which are the images taken during takeoff and while the plane gains enough height to start its flight over the study area according to the flight planning already created, and the last pictures which are clearly during plane landing.

The next step in the cleaning process is to determine what was the study area already planned before, and delete all the pictures taken out of the study area while the plane is curving to return to the planed flight lines. A good strategy is to identify where the straight lines are starting to break, and where the orientation angles are getting greater than during the normal flight line. After all of the correct images are selected, copy the image file paths from the feature table, and create a CSV file with it, to be used later, called BlockXX.csv(XX for the number of the block created).

Block Creation

The 2d3 Altimap is designed to process up to 250 to 300 images taken from SUASs as stated by its developers. To evaluate this capability, an experiment using

Sea Horse Island in Cedar Key was done. The mission was on the North side of the island. It's an area approximately 1,500 meters by 360 meters or a total of 330 images after cleanup.

The flight plan was executed in a back and forth pattern; flying east to west on strip one (farther south) and returning from west to east on strip two. This pattern was repeated for five lines, where the pass returned on the same line. For this experiment only the downwind flight path was used on strip five, considering for worst case scenario data with less overlap percentage. Then the pattern continues from strips six with east to west bound until strip thirteen with a west to east bound. The first 9 strips, which are around 260 meters in the north direction, are around 1,500 meters long. The last 5, around 100 meters wide, are 1,100 meters long. This is done like these because of the configuration of the island of the study area. For this dataset the average side overlap is 65% and forward overlap ranges from 40% in downwind strips to 80% in upwind strips.

For this experiment, 4 different block configurations were created to get different scenarios (number of strips, number of total images, overlap, features on final mosaic). Configuration 0, which is the entire image set of the study area; configuration 1, the division of the 13 strips into 3 blocks of 5 strips each, keeping one common strip between adjacent blocks to leave certain overlap between blocks; configuration 2, using two rectangular blocks, depending on the length of the different strips, leaving the first 9 strips which are 1,500 meters long, and a second block with the last 5 strips adding strip number 9, with their approximate length of 1,100 meters long; and configuration 3, which the block was created from northeast to northwest then moving southeast to southwest. This was to create more potential similar geometries and image quantity

between blocks, using primarily 5 strips on the vertical direction, and approximately 9 images (upwind direction) on the horizontal direction, the final block was approximately 380 meters by 130 meters, 3 on the top tier, 4 on the middle tier and 4 on the bottom tier, 11 blocks in total. Block Configurations of Sea Horse Key Mission are shown in Table 4-1 and Figure 4-1.

Total Processing Times

After adding up the total time of processing for every configuration (See Table below), the total time of processing is similar for every configuration. This favors creating just one block of data for the study area with datasets similar to the one used for this experiment with specifications described above. Due to the data preparation time for every block, it greatly reduces total processing time creating the one block instead of a block per certain amount of square meters that would be the other option. Table 4-2 shows total processing times for all configurations.

Processing Time Results

The processing time for every block ranged from a few minutes to close to 20 minutes (As shown in Table 4-3), which gives this software a reasonable time for processing mosaics. With this amount of time, the UAS can be deployed and extract the data from it, and the entire mosaic processing can be done in around one hour including the data preparation explained above. Which makes it very convenient for almost real-time monitoring of cases that need a really fast aerial image assessment (like disaster assessment or emergency monitoring).

Block32 and Block35 weren't able to be processed to a mosaic due to the complexity of the features in them such as water with waves. The program ran for less than one minute in each case, helping us by knowing that when a mosaic does not have

enough image pairs to create a mosaic, it will not try to match the image indefinitely. Block0 is also on the table, which is the Block that had the entire Strip 9 flown twice both downhill and uphill, so we can evaluate this block in processing time for total image count before processing.

By comparing total images contained in each block versus processing time (See Figure 4-3), we can see there is no a true correlation between images and processing time. There is certain relationship, accounting for a big difference in image count, but not a true one. The user can not say from the beginning, I have X amount of images so this will take X amount of time to process, and could be able to decide on going for bigger or smaller blocks accounting with that specific number. A value of total processing time per image was calculated on Table 4-3, showing again the lack of relation between these factors.

This lack of correlation explained above is notable even in blocks with the same number of strips, or the same amount of overlap percentage, or even same amount of images. On Figure 4-4, it can be seen that from Figure 4-3, but zoomed in to Block Configuration 3, where it shows an entire non correlated result all over the chart. This result is perhaps because, when taking smaller blocks, the blocks had only one feature in them (water only, bare ground only, vegetation only or grass only). Unlike bigger blocks that probably contained all features (water, bare ground, grass and vegetation) in them, making them easier or harder to be matched by the software. Figure 4-5 is another example of the lack of correlation between overlap percentage and processing time. This time the chart is divided in the different Block Configurations, because here

only blocks with similar numbers of images can be compared to others regarding overlap and time.

On Figure 4-6 and Figure 4-7 there is enough evidence that the final output size or quantity of images matched in the final mosaic has a great relation with processing time. Unfortunately, this is not good for stating a good idea from before the process on the quantity and size of blocks to be created for the processing.

Maximum Quantity of Images Processed by 2d3

To establish the maximum number of images that can be processed, there was another mission adjacent to this 13 strips of data, to the south (south side of the island), and one strip was added to the 13 original, with approximate of 1,500 meters long each, for every run, the software worked well until the number reach 600 images, after that the software started to create wrong shaped mosaics, as shown on Figure 4-2, and after 650 images it started crashing due to high number of calculations.

Import Exif Data to Images

Exif, Exchangeable image file format, is a standard that specifies the formats for images, sound and ancillary tags used by digital cameras, scanners and other systems handling image and sound files recorded by digital cameras. Almost all new digital cameras use the Exif annotation, storing information on the image such as shutter speed, exposure compensation, F number, what metering system was used, if a flash was used, ISO number, date and time the image was taken.

The Exif format has standard tags for location information. In these days a growing numbers of cameras and mobile phones have a built in GPS receiver that stores the location information in the Exif header when the picture was taken. Other cameras that don’t have a built in GPS receiver are not compatible with a separate GPS receiver that

can be adapted to the flash connector and can write the same geolocation information to its images. For other cases users can add to any digital photograph manually or from a handheld GPS receiver to the images taken with digital cameras, this process is known as geocoding.

To start the CMD script to prepare to work with 2d3 Altimap, 2d3feeder.py, the first step is to write the Exif data to the images. In order for this to work, we have to make sure on the geotags.csv file, parsed from the log file, that there is no negative elevation. This geotags file already has the original directory where all the images are located. So the CMD script will automatically write the Exif info on the original images; longitude, latitude, height, and orientation data. Figure A-1 and Figure A-2 show webpages that can be used to read the full Exif data, and also shows on Google Maps the location of the image, like exifdata.com or http://regex.info/exif.cgi/exif.cgi.

Creating Image Directory

On this step of the data preparation, the hard work is already done on the data cleaning process. The next step is to subset al.l images to be used to a new directory, which is done with the geotags.csv file created on the cleaning process. This file contains nothing more than the image file path. It will create a new directory at the location we select, to be called Blockxx (xx is the number which the block was called).

Processing

After the images with the Exif info have been written to the new directory, everything is ready for post processing. Now a scale and a desired output format need to be chosen.

Changing the settings can be done in the 2d3feedyr.py script, on the last line. First, change the scale factor from 0.1 to 1.0, the default of which is 0.25. To change the

output settings, just write the command that fits more with the desired output: --single, which outputs a single Geotiff image plus a KML wrapper; --tiled_kml, the output is a Geotiff tile set. Other processing options are an exhaustive image matching method and a bundle adjustment method.

Processing Report

The 2d3 software was the most difficult to use of the three software programs tested. It does not contain a user's manual or help menu. Also it is in a command line interface.

The software reports its processing steps and results, but this report comes in a DebugDump approach which can be found in the directory where the Altimap.exe file is located. This debug dump actually is every line written by the software during processing. It contains all of the coordinates read from images, the feature matching process, and rectifications.

Processing Time Assessment

The intention for this work was originally to do a time processing assessment and comparison between all software evaluated, but the LPS and EM software require manual user input in different steps of processing so it was difficult to quantify time in these programs. In 2d3 Altimap the software runs all the steps altogether and with no manual user input after the processing starts. A stopwatch was used to calculate the processing time for every block configuration, and to determine what type of relation there is between processing time and different specifications of the datasets.

The processing time has a direct relationship with the quantity of images on the block, as shown on Figure 4-8. This means that for constant features on the images, the total processing time can be predicted by considering only the image count.

Overlap Percentage Assessment

The intention of running the flight lines several times and in different directions was to get different scenarios of forward and side overlap percentages, and to evaluate the impact of these on UAS photogrammetry processing.

The images processed per minute ratio has no relation with different overlap percentages, as shown on Figure 4-9. In this figure, the side lap percentages were divided into two groups, 40% and 70%. With the side lap percentages fixed, the forward overlap impact of image per minute of processing is not related.

As mentioned before the photogrammetry mosaic processing is a multi-step process. 2d3 Altimap matches tie points within adjacent images, and even though 2d3 does not detail every single tie point, it does give results on pairs of images matched. To visualize the difference that forward overlap percentages have on image pair matching, a scatter plot is shown on Figure 4-10, where a clear increase of forward overlap means an increase in pairs correctly matched. We can see that with a greater side lap percentage, there is a greater percentage of image pairs matched, showing a strong impact of overlaps in the image matching technique used by 2d3 Altimap.

Finally the scatter plot on Figure 4-11 shows an increase in forward overlap means an increased percentage in images mosaicked.

Cloud and Tree Impact Assessment

Using the manual survey of all the images where percentages on tree and cloud coverage was created. To establish what the presence of trees or clouds in the datasets can do to change the mosaic processing, a percent of images with the presence of trees and the presence of clouds, and these were compared on each block to the percentage

of images mosaicked to see if an increase of images with trees or clouds means a decrease of images mosaicked percentage.

After an in-depth evaluation on Figure 4-12 the scatter plot does not show he expected results that the higher percent of images with trees or cloud will decrease the percent of images mosaicked.

EnsoMOSAIC

EnsoMOSAIC is an aerial digital imaging and image processing system which produces, geo-referenced multispectral image mosaics that cover large land areas. This software also has the hardware counterpart for image capturing and processing for users that need a system to start imaging and ortho-production.

EnsoMOSAIC UAV software reads aerial images taken with compact cameras carried onboard UAS, and processes them into seamless image mosaics.

The input requirements for the EnsoMOSAIC software are; the images, in any common format; GPS coordinates from the flight log in any autopilot model; and camera calibration and parameters which can be calculated in another Mosaic Mill software package called RapidCal. UAS2EM converts the flight logs from many of the commercial available UASs and on the market.

Also, as optional parameters, to the mentioned above are, the initial image orientation, which are the roll, pitch and yaw calculations for every image in order to increase processing speed and improve accuracy; and ground control points (GCP), which contribute to improve accuracy.

EnsoMOSAIC UAS processes automatically the images into ortho-rectified image mosaics, which have map coordinates and are thus GIS-ready and viewable immediately in Google Earth. EnsoMOSAIC applies photogrammetric principles, in

contrary to image stitching which is commonly used for UAS photogrammetry programs images. Stitched images are often visually pleasing, but contain distortions which are not suitable for area or distance measurements. EnsoMOSAIC does not stich, but rather it rectifies images into ortho-mosaics which are free of distortion in areas with elevation variations. This is possible because EnsoMOSAIC calculates a DEM within the rectification process. Ortho-rectification creates ortho-photos and ortho-mosaics, which can be used in the most demanding topographic mapping projects.

Mosaic Mill

MosaicMill is Finland based technology company established in 2009. The development of EnsoMOSAIC tools was started in co-operation with Technical Research Center of Finland and is today being continued by MosaicMill with its partner companies.

EnsoMOSAIC UAV and EnsoMOSAIC 3D are software solution for UAV image rectification and DTM and DSM processing. EnsoMOSAIC is also a turnkey imaging solution for manned aircrafts containing a complete set of software, hardware and support components.

Input Data

EnsoMOSAIC requires that digital images have GPS coordinates recorded in the aircraft or estimated with maps. Camera (or aircraft) exterior orientation parameters are not required but if they exist the rectification process is faster. Most common image formats are accepted.

For the data input and preparation, we should define a few concepts. Area is a geographically limited area of operation, they are mostly continuous and contain a single block of images. Areas can also consist of more than one block of images. A

block of images within the area, there can be one or several block in one area. A block can be divided into sub-blocks, this is recommended especially if the main block is large, when computer capacity may restrict image processing. The block adjustment may be slowed down, if the number of images in one bloc is too large for the capacity of the processing computer.

Current day computers rarely require division of blocks into sub-blocks for processing. It is recommended to process any block as a single calculation unit. The processing productivity depends on the computer capacity, number and type of images in a block, spectral and pixel selection settings and method used in the mosaic formation. The maximum number of images that can be processed simultaneously varies, but with modern computers of 2-4 GB of RAM image blocks of tens of thousands frames are manageable. The limits can be found by empirically testing in each computer setup. Blocks larger than the computer limit should be split into sub-blocks and processed separately. A sub-block should have a regular form as possible, since irregular shapes may lead to unwanted rectification results. Overlapping surface must exist between adjacent sub-blocks in order to facilitate their re-joining.

Creation of Blocks

In order to use the correct image data to be processed in EnsoMOSAIC, the dataset has to go through the similar data and image cleaning process as 2d3 Altimap and Erdas LPS. The images captured at the ascending and descending times should be erased, and the images captured on the turn back process while taking the next strip on the flight.

The first step in the EnsoMOSAIC processing block is the stage in the mosaic formation for a new area; three essential files have to be created in order to use it in the

EM software, Block Project File (.trp), GPS File (.gps) and a Camera Calibration File (.cam).

TRP File

The first of the files to be created is the TRP File which is a block definition and master file, it defines the output and location of camera and control point files, and image file names by flight line. The TRP (.trp) file contains 8 header lines where comments, output projection, location and name of camera calibration file, location and name of the ground control point file, approximate mean ground elevation, rotation of the camera, background NCA and NCM map path and file names, location and name of background map files. After the first 8 lines, lines containing each an image and the following information: flight line number, frame number, image file and image directory. If the images are captured in raw formats in must be specified on this file. Camera rotation is in degrees counter-clockwise, in relation that the aircraft's nose is pointing. Zero (0) for no rotation, landscape mode; 90 or 270 is for rotated portrait mode; and 180 is for backwards landscape mode. There must be a data row in the GPS (.gps) file for each image listed in the TRP (.trp) file, the GPS file may contain more data rows than there are images in the TRP file.

GPS File

The GPS (.gps) file is an image GPS-coordinates and optional camera orientations file. This file contains variable columns, but the predetermined ones are as follow: Line number, frame number, longitude, latitude, altitude, heading, UTC date, UTC time, UTC year, yaw, pitch, roll and tilt tag.

Line and frame numbers must match those in the TRP file, longitude and latitude must be in decimal degrees southern and western hemisphere with a minus (-) sign;

altitude in meters; heading in decimal degrees taking N as zero (0) degrees clock wise to 360. The UTC date, time and year are optional and used in sun angle correction and to calculate automatic links, if omitted sun corrections and links cannot be calculated but all other functions are available. Tilt angles and tilt tag are also optional and if used the UTC date, time and year are also required. The EM convention for tilt angles are: yaw, clockwise positive degrees from 0 to 360; pitch, nose up positive degrees, nose down negative degrees; and roll, left wing up positive degrees, left wing down negative degrees.

CAL File

The CAL (.cal) file is a camera internal orientation and calibration parameters. This camera calibration file contains channel, focal length, principal point's coordinates, general scaling and calibration parameters obtained through a proper calibration procedure.

Pyramid Images

The first step in processing is creating the image pyramid layers, these enable fast image display and faster calculations, these pyramids are a principal component of the automatic aerial triangulation algorithm used by EnsoMOSAIC, for this step all pyramids were created including level 0 for original images.

Automatic v7 Aerial Triangulation

Automatic Aerial Triangulation is an algorithm used by EnsoMOSAIC that contains both tie point location and block adjustment altogether, it uses a measurement three-stage process: (1) initial, (2) intermediate and (3) final. The initial assumes that the exposure locations have some accuracy,that means that GPS observations were collected in flight. For the initial stage the software recommends to start at level 5, or

level 4 for lower format images, by trying several times to start in level 4 was better because enough tie points were found while in level 5 they weren't. The intermediate stage assumes that image positions and orientations are available, the first estimates of the orientations where calculated by initial stage. The intermediate stage is run from the next stage after initial stage down to level 0, as layer 4 was used for initial stage the intermediate stage was run individually from 3 to 0. The final stage was used to finish the calculations at the lowest level and to transfer the results from the lowest level to the main level. The variation of Root Mean Square Error (RMSE) per measurement stage is shown in Image 4-13.

The tie point assessment for EnsoMOSAIC was run for every block configuration using 150 pixel search area and 0.80 image correlation, the criteria to accept and reject tie points. These values were set similar to Erdas LPS, so a comparison between both can be done; the correlation limit of 0.80 was used because the EnsoMOSAIC needs more tie points per image than LPS (6 for every quadrant versus 6 for entire images).

Figure 4-14 shows that for higher overlap percentages the tendency was that more tie points were generated, a result expected, also more tie points were generated while the total images on the block increased as shown on Figure 4-15. The number of tie points per image was less than 10 for low overlap blocks and more than 30 for higher overlap percentages blocks.

The tie point generation accuracy was assessed using 10 manually selected random points and later evaluated to see if they were matching on the different images that were present. This result are shown in Figure 4-16, were not as expected forward or side overlap percentages had any relation with accuracy, the accuracies ranged from

10% to 90% of tie points right. Figure 4-17 shows the percent of the images that didn´t have enough tie points, have clouds present on them. Also the percentages of the images that had pitch or roll values higher than 5 degrees are shown on Figure 4-17. According to these values, the images not used had considerable more clouds than high pitch and roll values in them.

If after the first tie point search the blocks did not converged, different search criteria was used, including changing tie point options and the spatial location of tie point search, when the triangulation converged, a review of residuals was done and higher residual values were deleted, as were higher altitudes and lower latitudes. A block adjustment had to be done after deletion of points, then more deletion of higher residuals, higher altitudes and lower altitudes until residuals less than 10 pixels were reached and altitude levels as expected, (20 to 30 meters for this dataset), when this was done, another block adjustment was done and the next measurement stage was later run, as described earlier, this is done until the final stage was complete.

Figure 4-18 shows that overlap percentages had no impact on Root Mean Square Error (RMSE) after Aerial Triangulation converged. Figure 4-19 show that in most cases for higher quantity of images used, the higher RMSE values were, meaning that when less images were used for mosaicking the more accurate the Aerial Triangulation process was.

Ortho-rectification

After the triangulation converged, the ortho-rectification process involved 2 steps: (1) DEM derivation and (2) ortho-mosaic formation. The DEMs created had pixels of 5 meters on the side. The ortho-mosaic was created out of original images, the preferred option for imagery collected with digital camera. DEM created previously was used for

the mosaic resampling, as it practically always improves the mosaic quality. The mosaic was created using the entire area, and a spatial resolution of the mosaic introduced was 0.05 meters as estimated for the imagery collected with the Canon camera for the used flying height.

Erdas LPS

LPS is a software application for performing photogrammetric operations on imagery and extracting information from imagery. LPS is important because it is a large commercial photogrammetry application that is used by numerous national mapping agencies, regional mapping authorities, various DOTs, as well as commercial mapping firms.

LPS is an integrated collection of tools that enable the user to transform raw imagery into data layers that are to be used in digital mapping, GIS analysis and 3D visualization needs. LPS provides support for air, space and terrestrial sensors. LPS handles triangulation and ortho-mosaic production, broad area mapping, transportation planning, engineering and facilities mapping, defense applications and close range applications.

LPS photogrammetric and image processing algorithms for automatic point measurement, triangulation, automatic terrain extraction and sub-pixel point positioning help improve accuracy while simultaneously increasing productivity.

LPS supports a wide array of workflows, processing imagery from a variety of sensors. With highly flexible, easy to use tools, LPS supports the creation of photogrammetric data products for a variety of purposes fluctuating from GIS to precision engineering applications (Erdas, 2011)

Erdas ImageStation

ImageStation is a software that enables digital photogrammetry workflows, including projection creation, orientation and triangulation, 3D feature collection and editing, DTM collection and editing, and orthophoto production using aerial and satellite imagery. It differs from LPS that is designed for high-volume commercial photogrammetry and production mapping users who need to move large quantities of raw information to an actionable or exploitable format. This software may fulfill the characteristics of UAS, that because lower flight altitudes, more images are acquired for specific areas than conventional airplanes.

Erdas

In 2010, ERDAS' parent company, Hexagon, acquired Intergraph. Both Intergraph and ERDAS have rich histories as pioneers in the geospatial software business, with Intergraph established in 1969 and ERDAS in 1978. ERDAS led the way with image processing and raster handling, the ability to maximize the pixel. Intergraph built a vector based strategy to build databases of geospatial intelligence. ERDAS and Intergraph are now a unified business as a result of the Intergraph acquisition (Erdas, 2011).

Image Cleaning and Input Files

In order to use the correct image data to be processed in LPS, the dataset has to go through the similar data and image cleaning process as 2d3 Altimap. The images captured at the ascending and descending times should be erased, and the images captured on the turn back process while taking the next strip on the flight.

The next step in the data preparation is the software input file, which the NOVA payload is design to output the data how the LPS reads it in a CSV .csv format. The

way the data should be organized by columns is: ID, which is image number; Path, where the image is located in the computer; longitude, in degrees; latitude, in degrees; altitude, in meters; omega, in degrees; phi, in degrees; kappa, in degrees. The rotation angles convention should be as in Figure 3-3. This file should be converted to DAT (.dat) Format, supported by the software.

To check if the orientation angle convention are right, a good practice is to turn on 2 images and add manual tie points, and find ATPs, if the found tie points are not correct that means that the orientation parameters are wrong, and omega, phi and kappa values should be checked, and rotate.

After the images were cleaned and the input file is created, the next steps were to (1) create a block in the software, (2) check the coordinate systems (3) add the sensor used (an Olympus E-420 DSLR), (4) add the camera calibration parameters. For this research, the camera had a focal length of 25 mm and focal point of coordinates on the center (0,0) of the image.

In the interior orientation option, open the Dat (.dat) File input file created. The size of every pixel should be changed in the interior orientation parameters in the Cell Array workspace to 4.74 micrometers on each side. The images should be represented on real coordinates on the map if, that is the case the Interior Orientation is correct.

Perform Automatic Tie Point Generation

After confirming the images on right place in the map space, the next step is to conduct an ATP generation. In the ATP search, the tie point could be by Exterior Orientation and or Ground Control Points, or by Tie Points already generated; search area, initial accuracy, and matching coefficient and point density; also the pattern can be selected for the creation of the automatically generated tie points.

Initial accuracy displays the relative accuracy of the initial values used by the ATP process, although the default value is 10%, the developers recommend a 25% if the exterior orientation option was used for initial type. Feature point density displays the feature point density percentage based on internal default, this value was tried for 10%, 50% and 100% in the Tie Point Generation Experiment to be explained next.

Other options are the existing point transfer, which can be changed from “No Transfer, New Points Only”, “Transfer Only, No New Points” and “Transfer With New Points”, I will play with this options when I need them, to re-do a ATP generation when not enough points were found for some images. Other options that were kept in their default value for this work Correlation Size (7 x 7), Default Distribution (5 x 5), Defined Pattern (Default Off), Intended Number of Points / Image (Pattern), Keep All Points (Off), Starting Column, Column Increment, Starting Line, Line Increment.

Tie Point Generation Experiment

To establish the better options a small experiment was conducted, using the block configuration 1, the ATP function was run several times using different search area criteria (See Table 4-4), point density percentage and initial accuracy values. An analysis was conducted evaluating the quantity and accuracy of tie points with every configuration, in both grass area and the forest area. 10 manually selected random points were taken from the grass area and 10 manually selected random points from the forest area, all 20 points were evaluated to see if they were matching on the images that were present.

On the non-vegetated area almost every configuration used was more than 90% of the points correct, making the ATP Generator very precise to finding points in non-

forested areas, while on the forested area the percentages were from 0% to 40%. (See Figure 4-20).

After conducting the experiment, there was not really a correlation between percent of rights points and number of points found. The chosen options for ATP generation for the assessment of LPS will be Search Area: 150 pixels, Coefficient: 0.9, Point Density: 10%, Initial Accuracy: 25%, this was the solution that gave the most auto tie points possible without giving away accuracy. (See Figure 4-21).

Auto Tie Point Generation Assessment

After the tie point generation process, the auto tie summary dialog opens to display the tie point generation for each image in the block file. After a quick review, a few of the points where checked to ensure accuracy, adjusted in the case of possible adjustments, and deleted if the tie points were completely wrong. Figure 4-22 shows that tie point generation accuracy did not change with forward or side overlap percentages.

Figure 4-23 shows that there is a direct relation between tie points found and overlap percentages, for higher percentage values more unique tie points are found automatically. Also, a relation is shown on Figure 4-24 between tie points found and total images in the block. Figure 4-25 shows the percent of the images that didn´t have enough tie points, have clouds present on them, the percent of images with cloud that were fulfilled were higher than 60% making this one of the reasons that this images were bad tied together. Also the percentages of the images that had pitch or roll values higher than 5 degrees are shown on Figure 4-25, being these considerable lower than the cloud impact (30% to 75%).

Aerial Triangulation

After the tie point generation and check, and all images had 6 needed images to proceed, the next step was performing an aerial triangulation, to adjust the final values of the initial approximations to exterior orientation parameters provided by airborne GPS and INS techniques. The technique used for projects with more than 2 images is the bundle block adjustment, as space intersection and space resection techniques cannot be performed. A bundle block adjustment as defined earlier is computed including exterior orientation parameters, X, Y and Z coordinates of tie points and GCPs in some cases, all the images are processed in one solution. A least square adjustment is used to estimate the solution for the entire block while also minimizing and distributing the error.

The options in the aerotriangulation dialog box, maximum iterations which I will use the default 10, a convergence value in meters of 0.10 meters as proposed by the developers, and the compute accuracy for unknowns will be used to calculate the accuracy for parameters such as exterior orientation, ground coordinates and other estimated by aerial triangulation, the images coordinates for reports in pixels as default., on the other option in the general tab, image point standard deviations will be left as default (0.33 x 0.33 pixels), and GCP type and standard deviation was not used, as GCPs were not used.

On the interior tab, the options were unchanged as any camera calibration was properly done. For the standard deviation for exterior orientation, a same weighted values for all images and the default values were used, 10 meters for X-Y-Z, and 5 degrees for pitch-roll-yaw, this values were left without change to try to establish a better perception of software capacities, trying to do it as more default as possible.

For additional parameter model, there are several models that can be used in aerial triangulation for the compensation of systematic image errors. The lens distortion model was used according to developers recommendation that this is especially effective with amateur digital cameras, this model has two additional parameters and is designed to self-calibrate the lens distortion parameters automatically. These additional parameters were used as weighted parameters, a small statistical weight value is assigned to each parameter automatically by LPS.

As a blunder error detection, the time saving robust blunder checking which uses a robust iterative weight function for gross error detection without computation of individual redundancy for each observation.

After running the software a dialog opens showing if a triangulation convergence was reached and total image unit-weight RMSE, if convergence was reached and the RMSE had an acceptable value, less than 5 in cases that were possible the results can be accepted and update the new exterior orientation parameters and proceed with the next step of the process, ortho-rectification.

To improve the triangulation results or if the convergence could not be reached, a review of the triangulation report and identification of the points with the most error, usually with higher residuals, and delete them from triangulation calculations. Other recommendation is to perform ATP generation using different options and configurations, and even doing manual tie point, in order to have more points, so a deletion of higher residual points can be made and the minimum points can still be have in each image, continue an iteration of tie point generation and triangulation until a correct adjustment can be done.

Figure 4-26 shows no relation at all between Root Mean Square Error (RMSE) and overlap percentages, and considerable higher values than resulting EnsoMOSAIC data.

Ortho-rectification

DTM Extraction

The DTM Creation is the first step in the ortho-rectification process, and between the different types of outputs, the one selected and more conventional file was a DEM, that is a raster file that depicts elevation in dark and light pixels; dark pixels represent low elevation areas, and bright represent high elevation areas, a single mosaic output file was selected, and it will take each DTM created by each image pair in the block and will be merged into one file, something similar to a mosaic. DEM Accuracy was left in default value, 25 meters, this is the tolerance in the vertical units of the terrain to set accuracy range for the predicted surface value of the area.

Ortho-Resampling

After the extraction of the DTM, the original images must be resampled orthographically. For ortho-resampling DEM previously created in the DTM extraction process was used. In this process the resampling method to be used was cubic convolution, no rescaling used, the whole pixels where aligned in overlapping images, and the resample was projected to UTM Zone 17 North projection, all other options kept as default, as overlap threshold,

In this process all images can be done together, to ensure that all output ortho-images have the same settings (for example, cell size, resampling method), set al.l of the options in both the General and Advanced tab before adding additional images to the process. Once these parameters have been set, they carry over to the additional images added to the list.

Mosaic Creation

MosaicPro was the application within Erdas and LPS used to join georeferenced images and form a larger image or a set of images. In this final step of the ortho-rectification process, when using ortho resampled images, not much decisions should be made, the only one is to set the overlap function, this one lets the user to set the intersection type and overlap function for the mosaicked image, the options are: (a) Overlay, the overlap area belongs to the image that is on top in the stacking order (b) Average, the value of each pixel in the overlap area is replaced by the average of the values of the corresponding pixels in the overlapping images (c) Minimum, the value of each pixel in the overlap area is replaced by the lesser value of the corresponding pixels in the overlapping images (d) Maximum, the value of each pixel in the overlap area is replaced by the greater value of the corresponding pixels in the overlapping images (e) Feather, the overlap area is replaced by a linear interpolation of the pixels in the overlap. A pixel in the middle of the overlap area is 50% of each of the corresponding pixels in the overlapping images. A pixel 1/10 of the overlap from an edge would be 90% one image and 10% the other. This was the option that worked better with the imagery used in this work.

Table 4-1. Sea Horse Key, Cedar Key Data Set Block Configuration.

Block	Images	Strips	Images/Strip Average (Images)	Min	Max	Height (meters)	Overlap Average (meters)	%	Min (meters)	%	Max (meters)	%
0	360	13										
00	326	13	25.1	17	34	173.4	57.0	52%	44.9	83%	75.6	37%
11	117	5	23.4	17	34	174.7	53.4	56%	46.3	82%	69.7	42%
12	133	5	26.6	20	34	174.3	58.3	51%	44.9	83%	75.6	37%
13	133	5	26.6	21	33	171.5	58.4	51%	46.2	81%	71.9	39%
21	117	5	23.4	17	34	174.7	53.4	56%	46.3	82%	69.7	42%
22	243	9	27.0	20	34	172.9	57.3	52%	44.9	83%	75.6	37%
31	45	5	9.0	7	12	174.9	53.5	56%	46.0	82%	70.1	42%
32	39	5	7.8	6	9	174.3	53.5	55%	46.2	82%	69.4	42%
33	37	5	7.4	6	9	175.2	54.3	55%	45.7	83%	71.2	41%
34	42	5	8.4	5	12	173.8	59.3	50%	45.5	83%	96.8	19%
35	36	5	7.2	6	9	174.3	57.7	52%	44.7	84%	71.6	40%
36	39	5	7.8	6	10	174.4	57.4	52%	44.2	84%	71.0	41%
37	30	5	6.0	5	7	174.9	58.0	52%	45.2	83%	70.4	42%
38	42	5	8.4	6	11	170.9	60.1	49%	46.2	81%	76.7	35%
39	38	5	7.6	6	9	171.9	59.1	50%	45.3	82%	71.8	39%
310	36	5	7.2	6	9	171.9	55.8	53%	44.8	83%	68.4	42%
311	31	5	6.2	5	8	171.6	57.6	51%	42.3	86%	74.4	37%

Table 4-2. Total Processing Time Per Configuration

Configuration	Blocks	Minutes	Seconds
0	1	18.92	1135
1	3	21.20	1272
2	2	20.63	1238
3	11	23.02	1381

Table 4-3. Processing Results

			Time		Seconds/	Connectivity		Image Pairs		Clust	Total Area	Macro	Tot
Block	Images	Strips	Seconds	Minutes	Image	Nodes	Edges	Matched	Tried	(Units)	(Pix x Pix)	Tiles	Ima
0	360	13	1230	20.50	3.42								
00	326	13	1135	18.92	3.48	326	479	479	911	2	648188274	52	202
11	117	5	236	3.93	2.02	110	77	77	281	2	137414976	14	38
12	133	5	426	7.10	3.20	133	158	158	346	3	269828425	22	75
13	133	5	610	10.17	4.59	133	270	270	349	2	347254765	26	118
21	117	5	258	4.30	2.21	110	77	77	281	2	137570539	14	38
22	243	9	980	16.33	4.03	243	417	417	671	2	507867918	39	177
31	45	5	88	1.47	1.96	45	25	25	112	1	53252220	6	13
32	39	5	23	0.38	0.59	39	8	8	99	0			0
33	37	5	125	2.08	3.38	37	48	48	89	1	77604402	6	23
34	42	5	125	2.08	2.98	42	47	47	105	1	74924232	6	21
35	36	5	23	0.38	0.64	36	13	13	90	0			0
36	39	5	167	2.78	4.28	39	73	73	98	1	99815296	8	32
37	30	5	115	1.92	3.83	30	32	32	74	1	83812663	8	18
38	42	5	190	3.17	4.52	42	79	79	104	1	119244796	10	36
39	38	5	206	3.43	5.42	38	56	56	95	1	102287625	8	25
310	36	5	173	2.88	4.81	36	82	82	90	1	110358024	8	36
311	31	5	146	2.43	4.71	31	65	65	77	1	82119555	6	29

Table 4-4. Configuration and Options Used for ATP Experiment

Configuration	Search Area (Pixels)	Coefficient	Pnt Density (%)	Initial Accuracy (%)
1	96	0.8	10	25
2	96	0.9	10	25
3	96	0.9	10	10
4	96	0.9	50	10
5	96	0.9	50	25
6	96	0.9	100	10
7	96	0.9	100	25
8	150	0.9	10	10
9	150	0.9	100	10
10	150	0.9	100	25
11	150	0.9	10	25

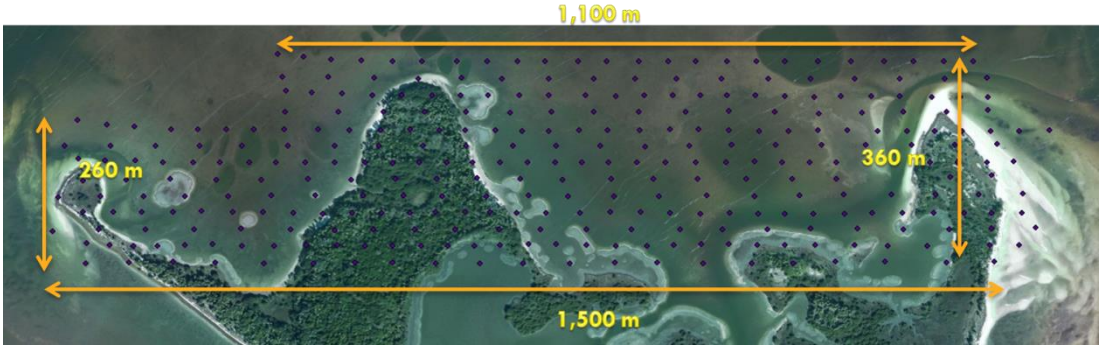

Figure 4-1. Sea Horse Key Data Set.

Figure 4-2. Scaling error after mosaicking a big number of images.

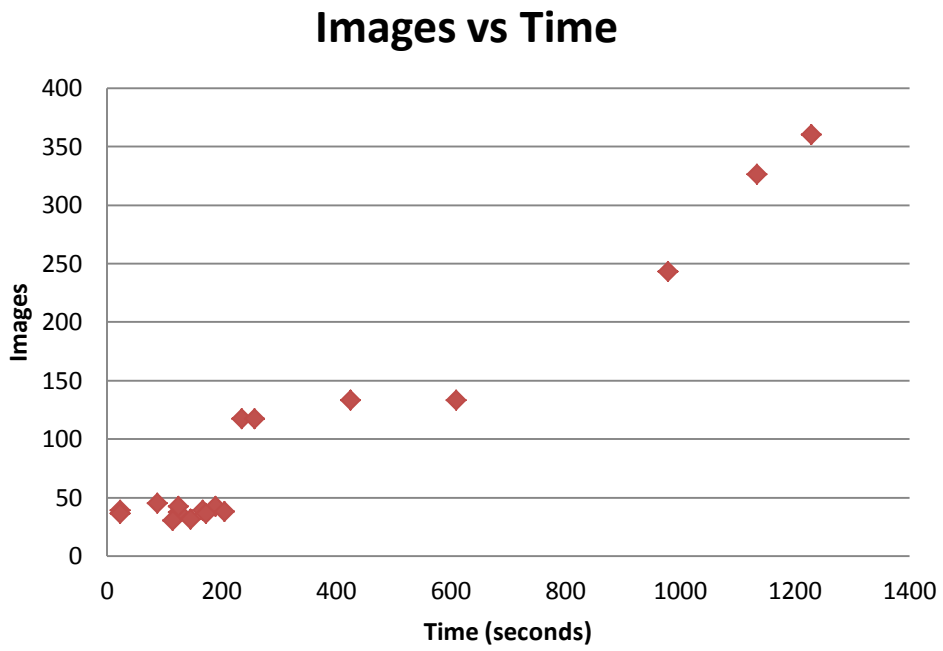

Figure 4-3. Images Processed vs. Time Processed Chart. Cedar Key mission data using 2d3 Altimap.

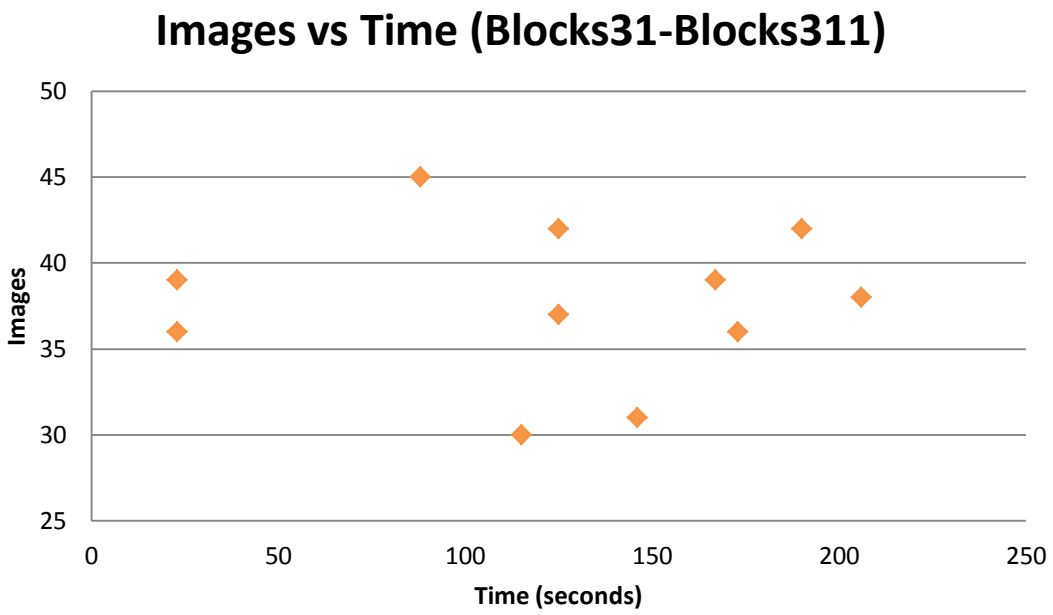

Figure 4-4. Images Processed vs. Time Processed Chart for Block Configuration 3. Zoom in to Figure 4-3 to the Block Configuration 3, showing there is no clear relation between number of images to processing time, maybe due to the different features contained for every final mosaic (water, vegetation, others). Cedar Key data using 2d3 Altimap.

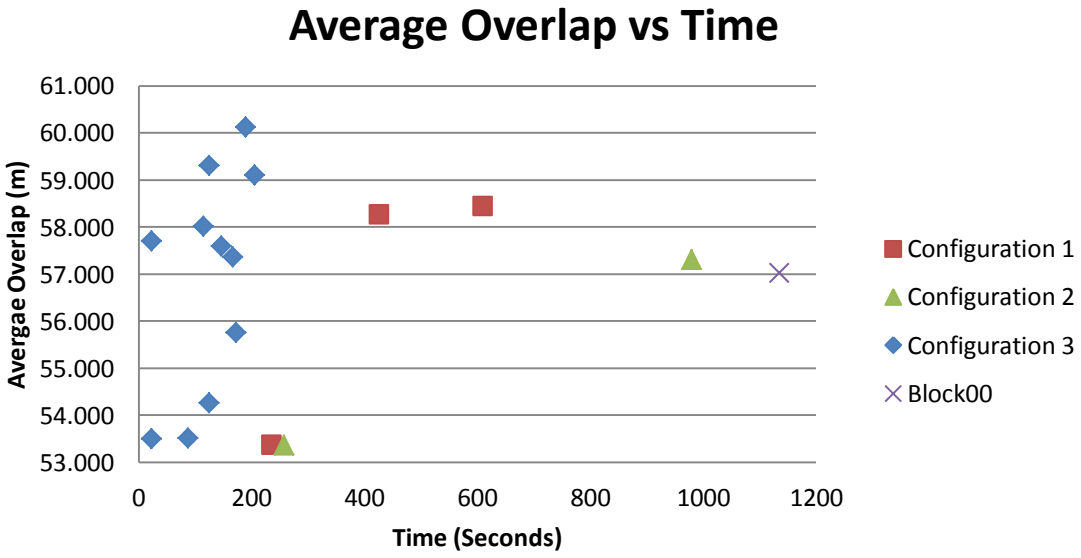

Figure 4-5. Chart showing the relations between average overlap to processing time. Every block configuration is represented with a different series to evaluate the true impact of overlap from block with similar number of images. Cedar Key Data using 2d3 Altimap.

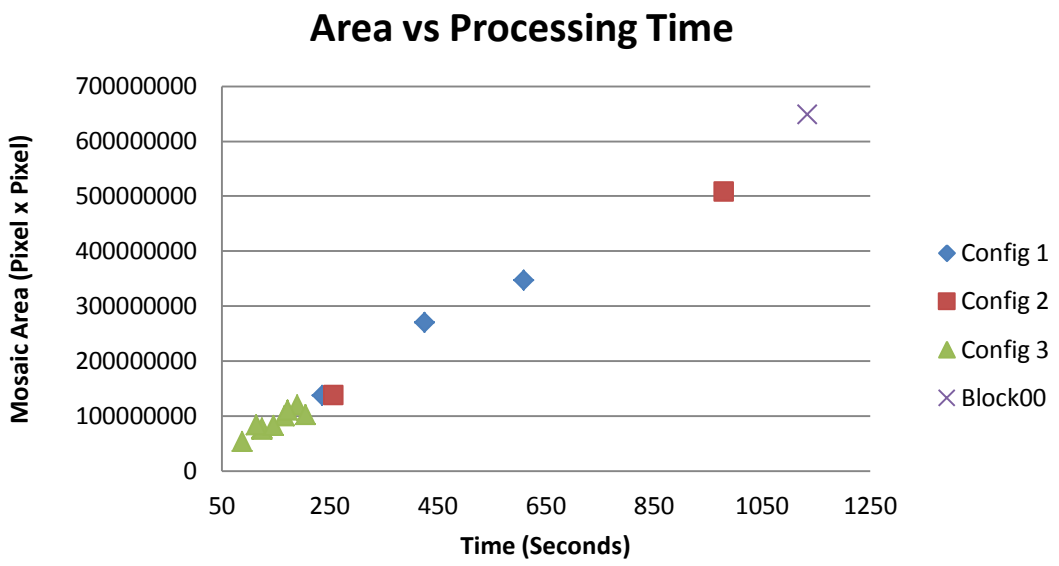

Figure 4-6. Relation between final mosaic area with processing time per block. The chart is showing a good relation mosaic area-processing time. Cedar Key data using 2d3 Altimap.

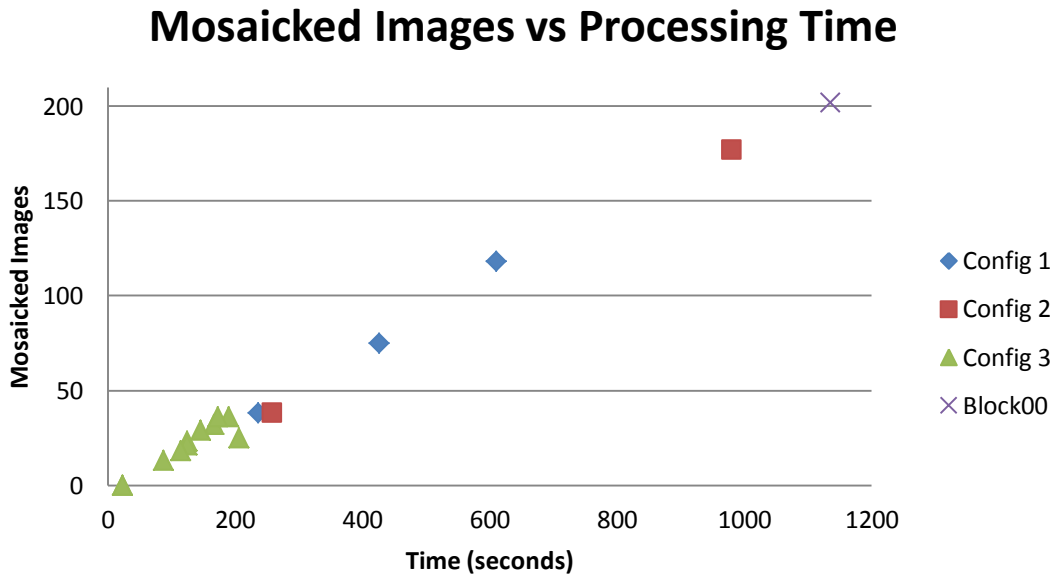

Figure 4-7. Relationship between number of images utilized in the final mosaicked product and the processing time. Cedar Key data using 2d3 Altimap.

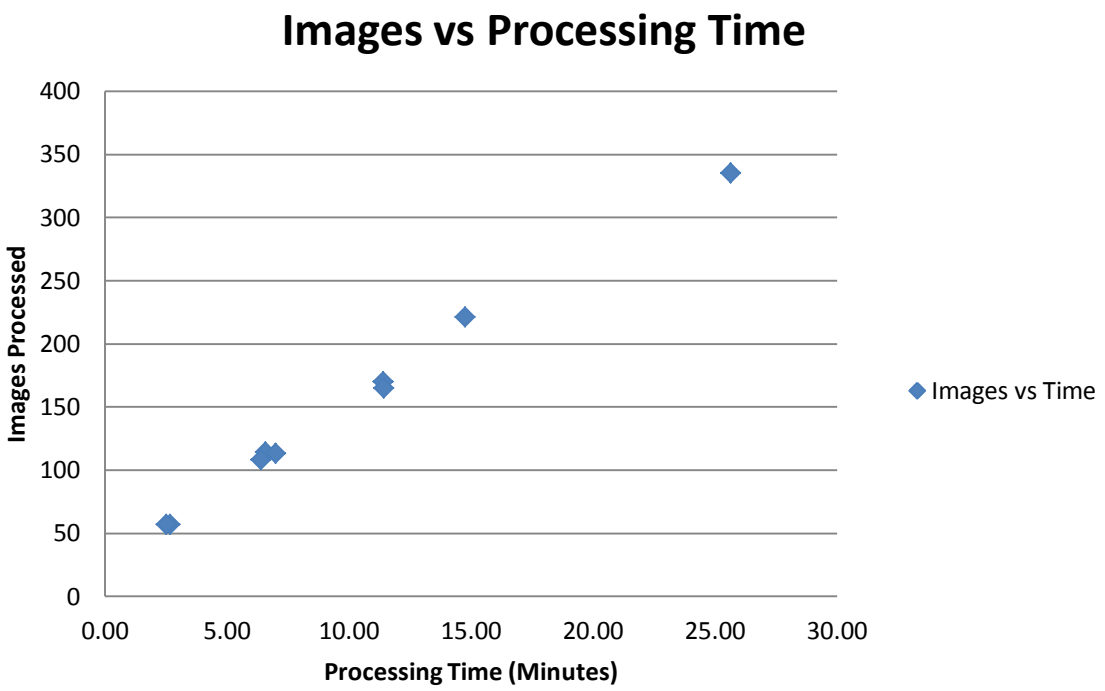

Figure 4-8. Relationship between Processing Time and Total Images in Block. Archer Fields data using 2d3 Altimap.

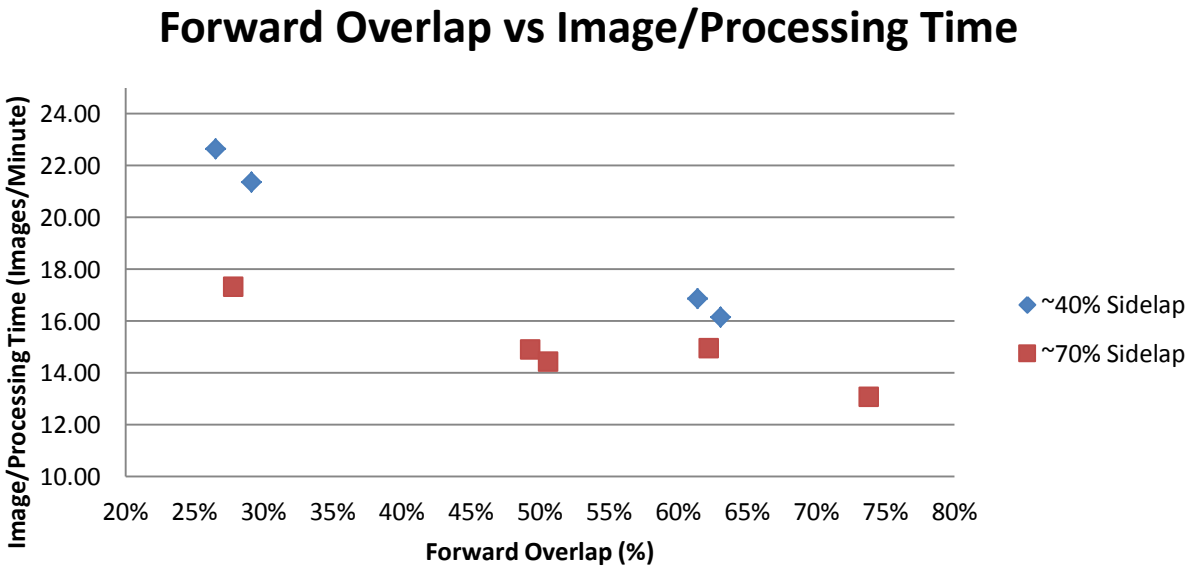

Figure 4-9. Relation between Image by Processing Minute and Forward Overlap. Datasets of 40% and 70% Side overlap. Archer Fields data using 2d3 Altimap.

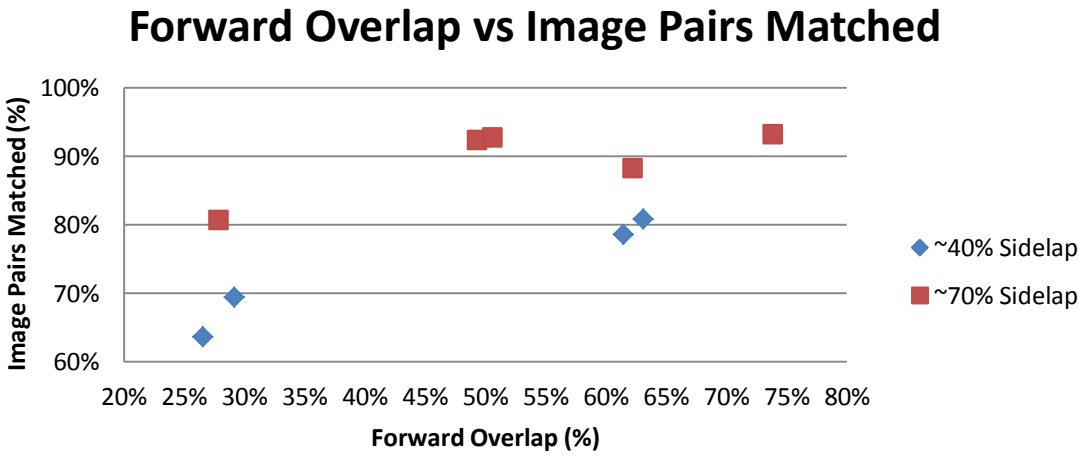

Figure 4-10. Scatter Plot Showing Relation Between Image Pairs Matched and Forward Overlap. Archer Fields data using 2d3 Altimap.

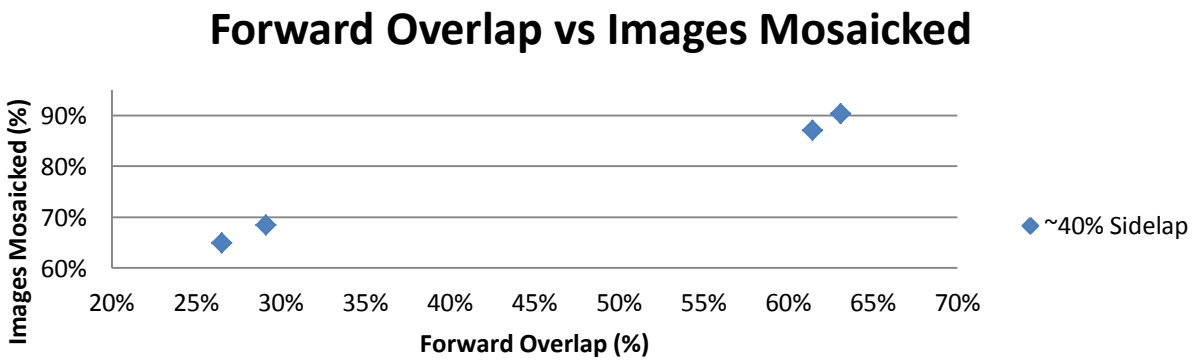

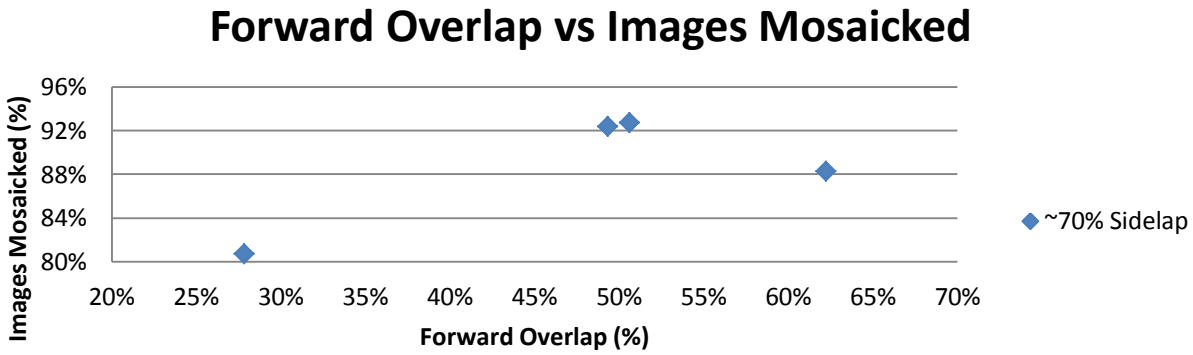

Figure 4-11. Scatter Plot of Relation Between Images Mosaicked and Forward Overlap. Archer Fields data using 2d3 Altimap.

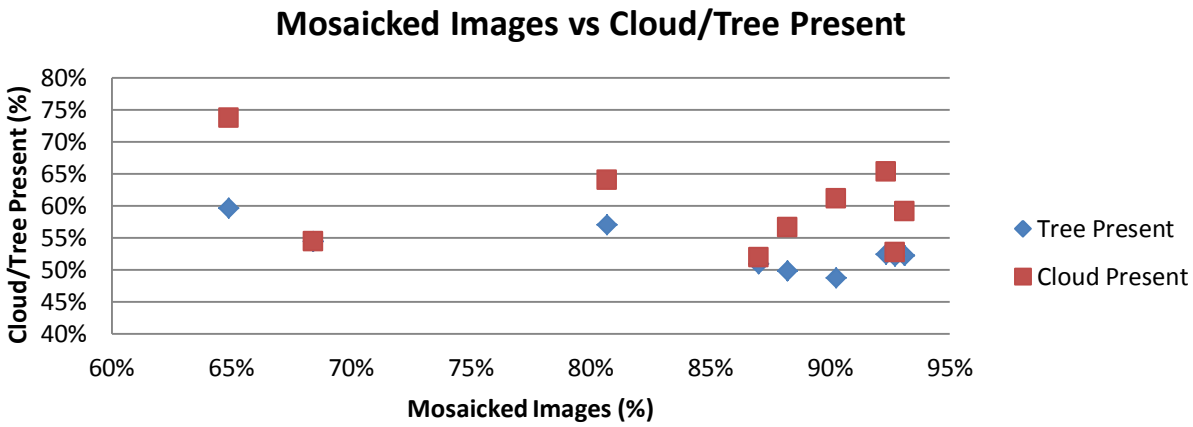

Figure 4-12. Scatter plot showing relation image percent with cloud and tree present. Archer Fields data using 2d3 Altimap.

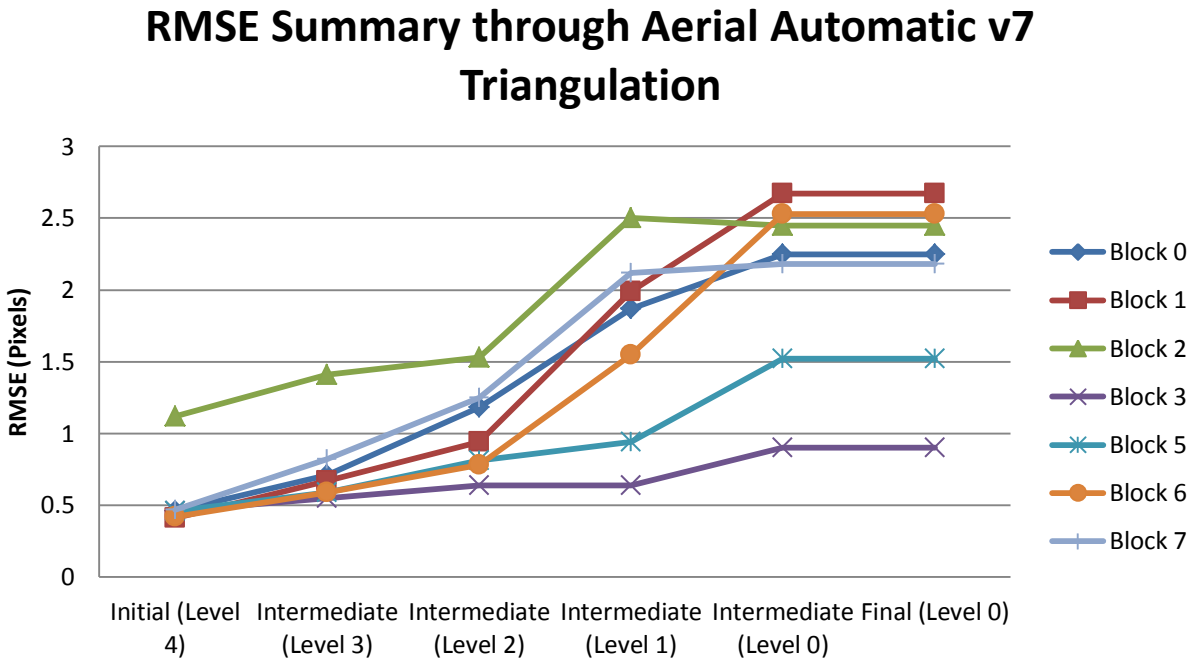

Figure 4-13. RMSE variation through measurements stages in Aerial Automatic Triangulation. EnsoMOSAIC.

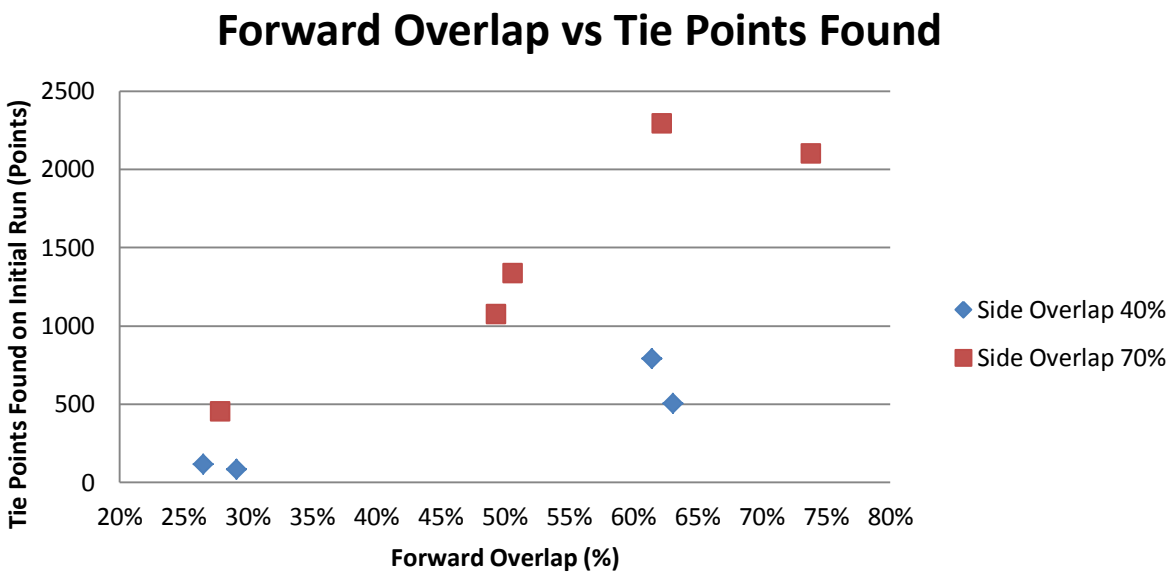

Figure 4-14. Scatter plot showing relation between overlap percentages with quantity of tie points found on the initial stage. EnsoMOSAIC.

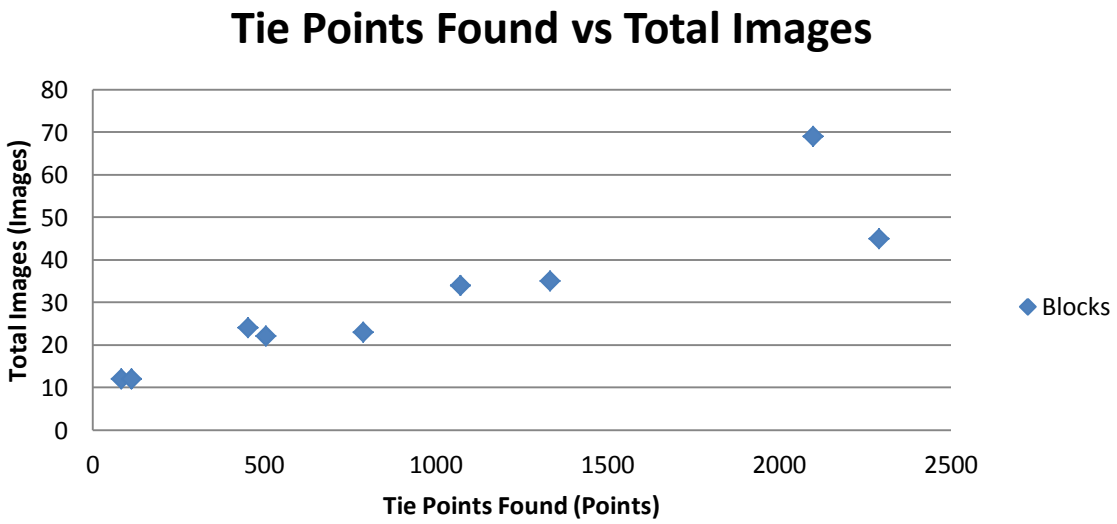

Figure 4-15. Scatter plot showing relation between total images in the block with quantity of tie points found on the initial stage. EnsoMOSAIC.

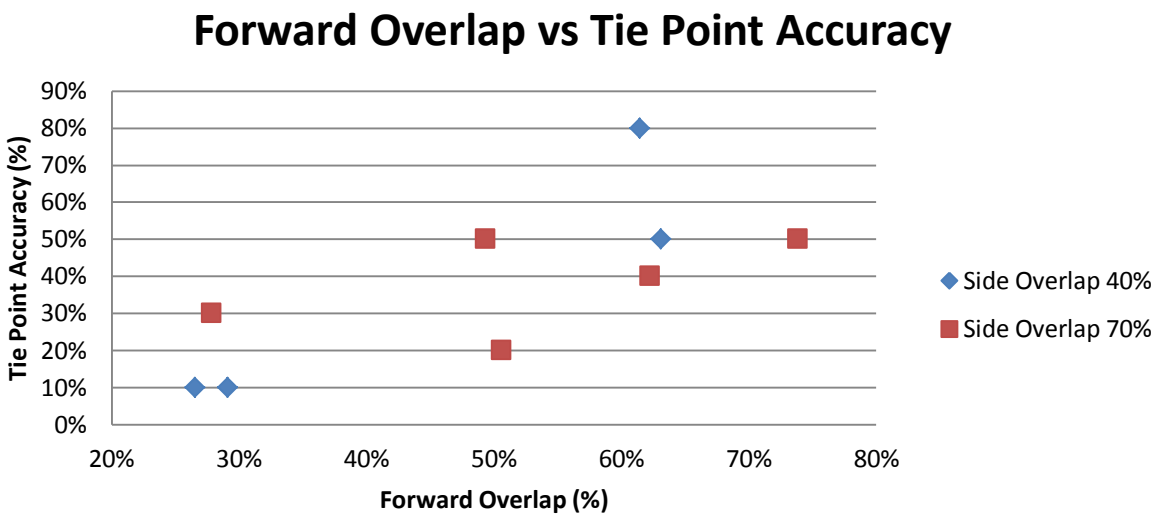

Figure 4-16. Scatter plot showing relation between overlap percentages in the block with accuracy of tie points found on the initial stage. EnsoMOSAIC.

.

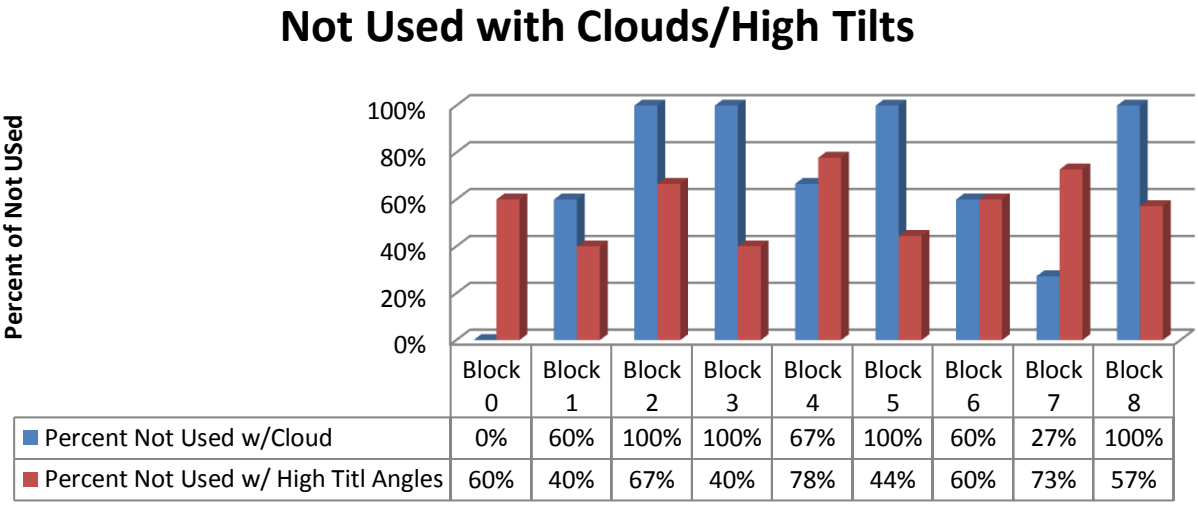

Figure 4-17. Cloud presence and high pitch-roll values impact on tie point search. EnsoMOSAIC.

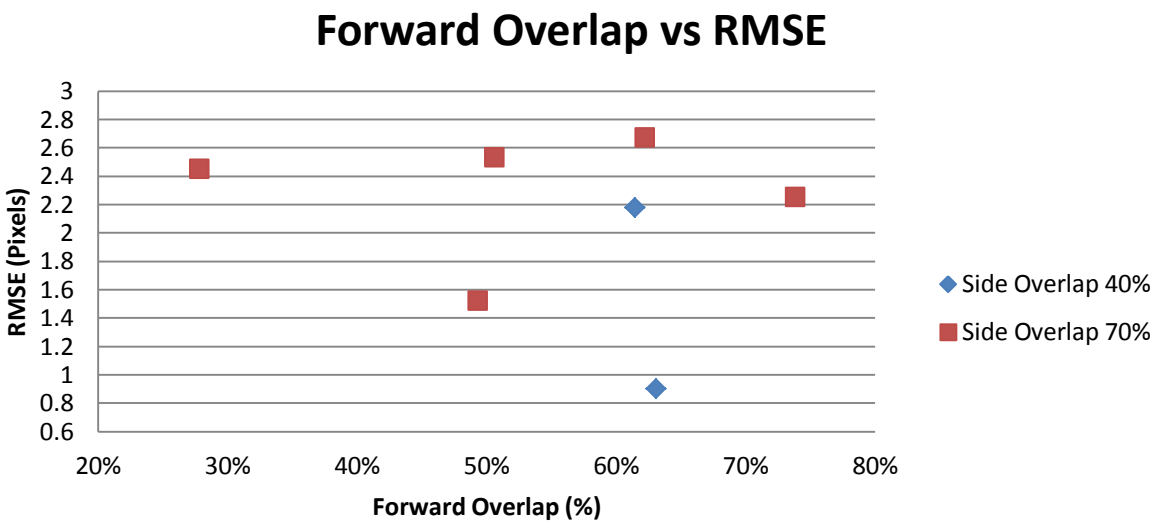

Figure 4-18. Scatter plot showing relation between overlap percentages in the block with Root Mean Square Errors on the Aerial Triangulation process. EnsoMOSAIC.

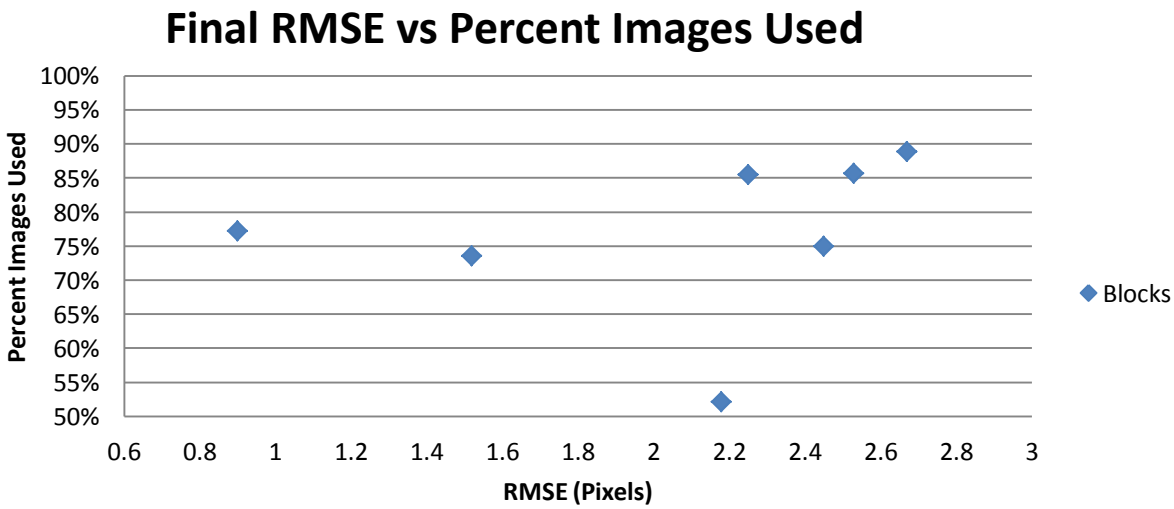

Figure 4-19. Scatter plot showing relation Root Mean Square Errors on the Aerial Triangulation process and percent of images used for mosaicking. EnsoMOSAIC.

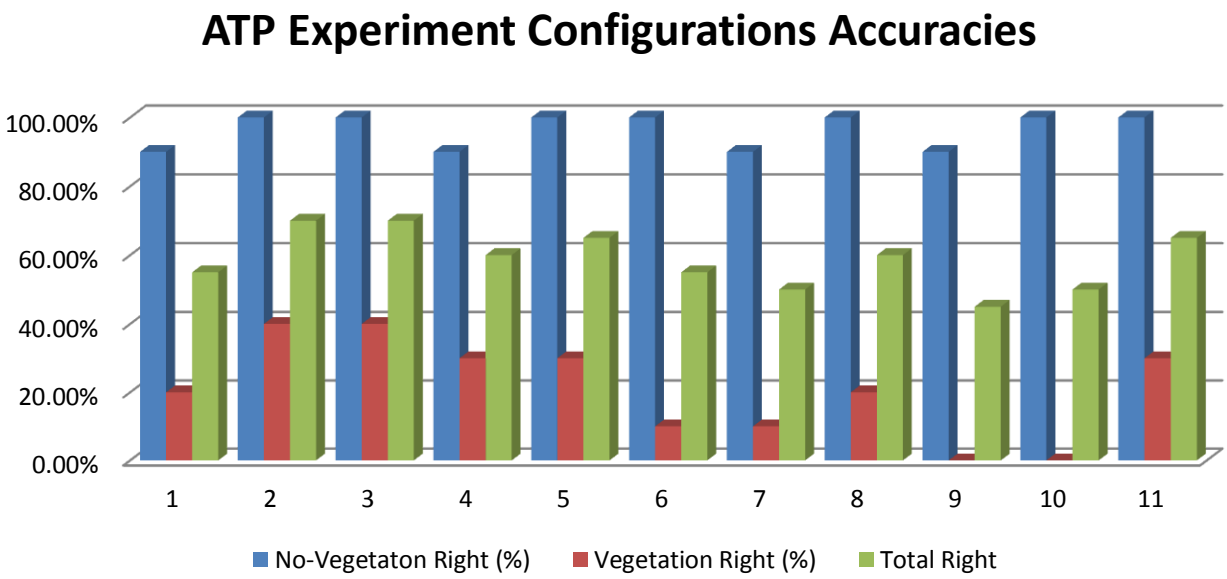

Figure 4-20. ATP Experiment Accuracy per Configuration. Erdas LPS.

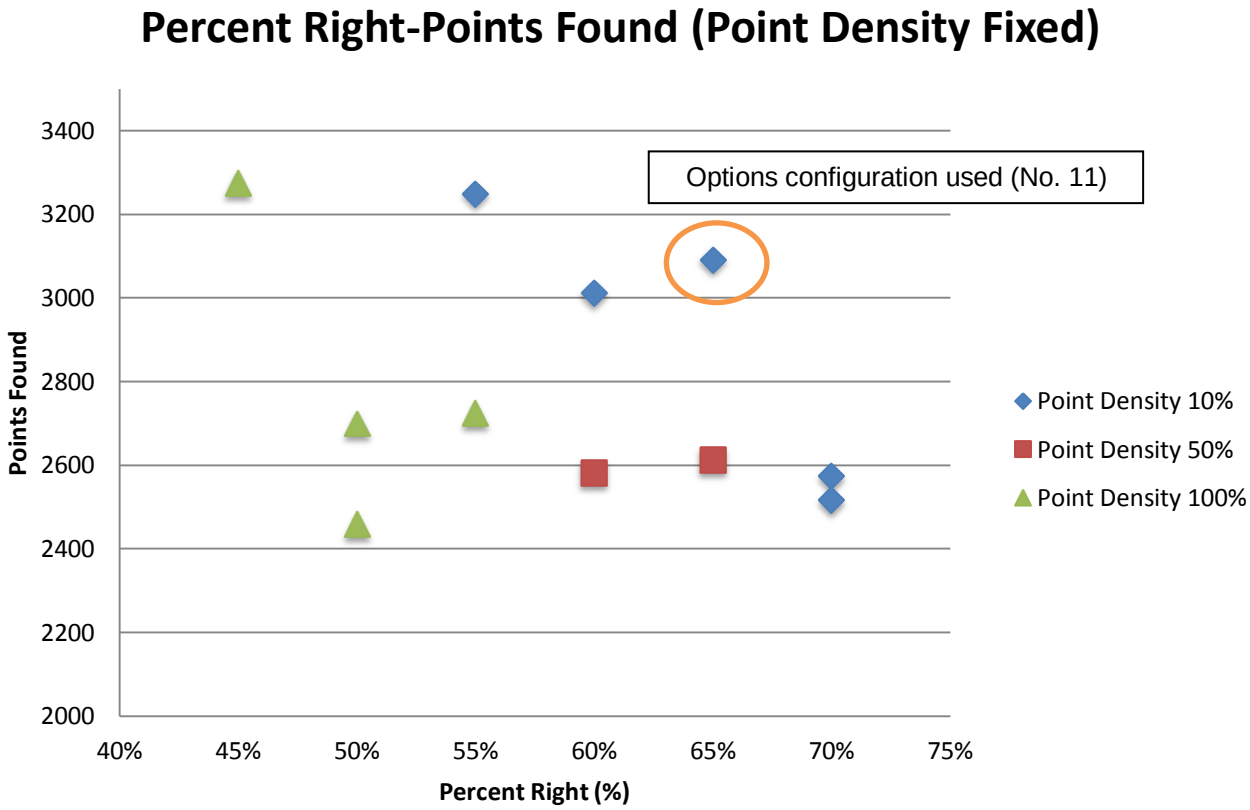

Figure 4-21. Scatter Plot Showing Percent Right vs. ATP Found. Erdas LPS.

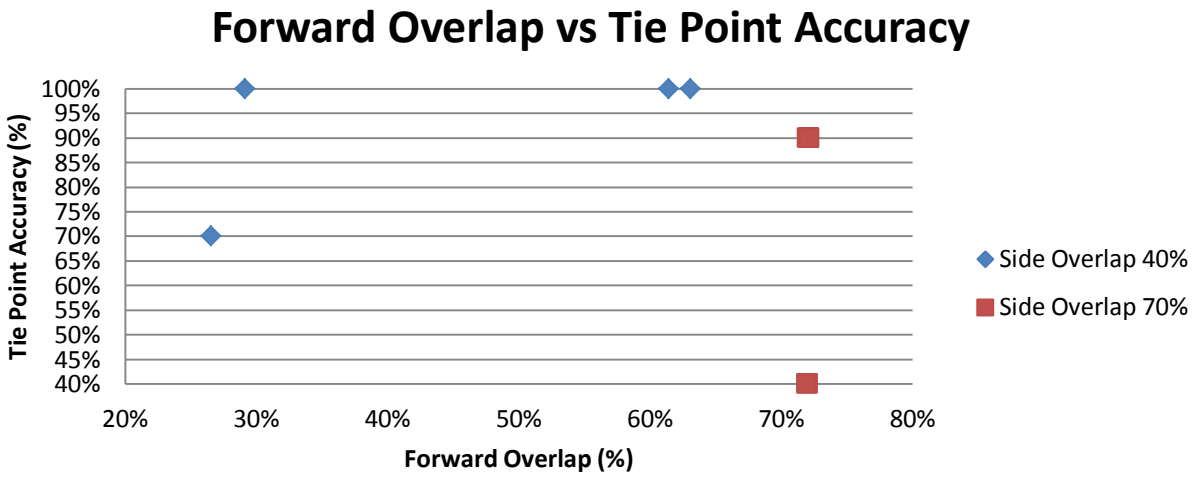

Figure 4-22. Scatter plot showing relation between tie point accuracy and overlap percentages. Erdas LPS.

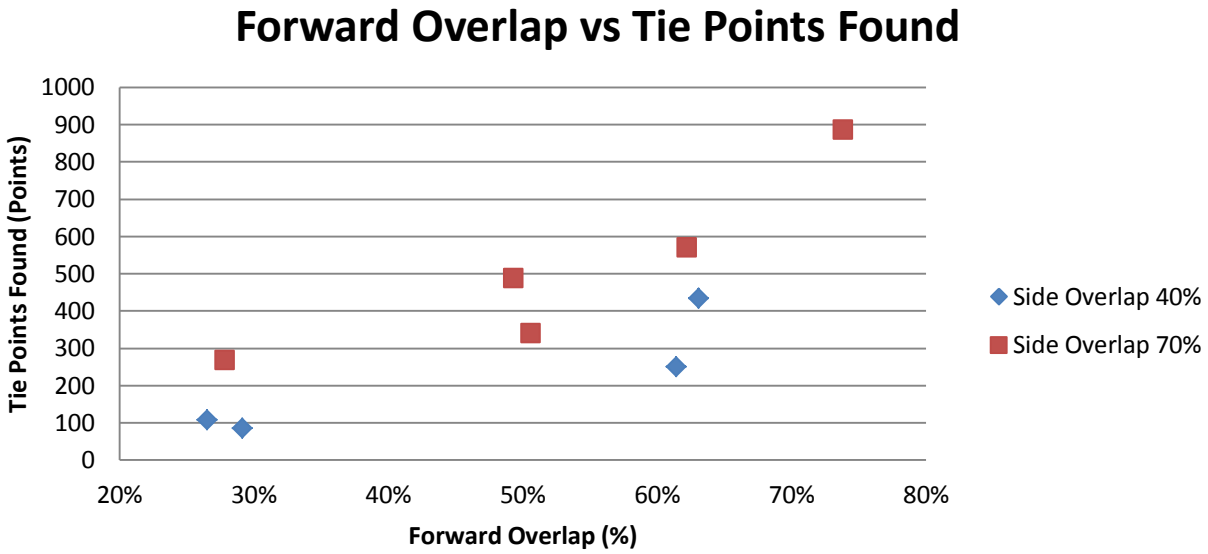

Figure 4-23. Scatter plot showing relation between overlap percentages with quantity of tie points found on the initial stage. Erdas LPS.

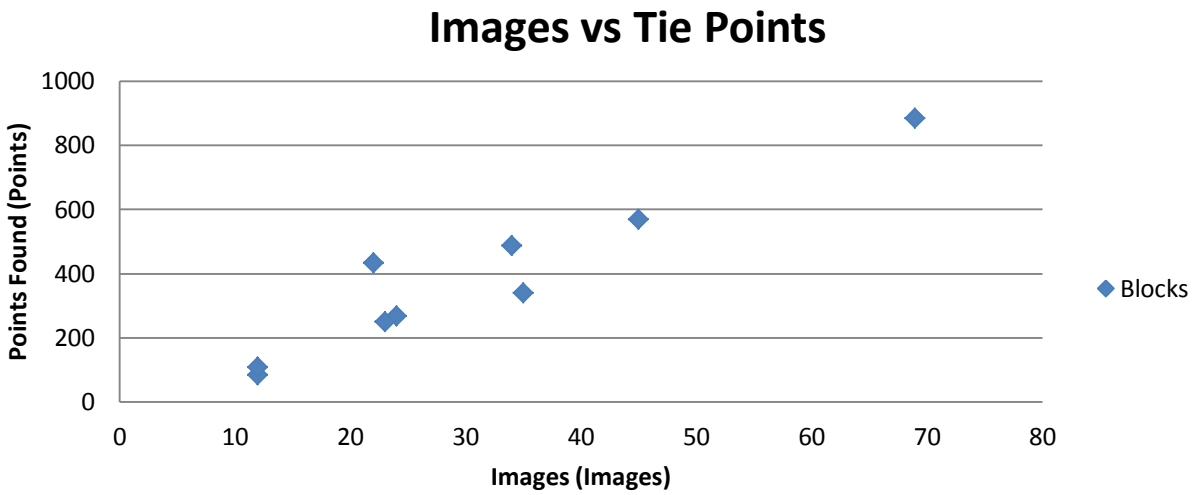

Figure 4-24. Scatter plot showing relation between total images in the block with quantity of tie points found on the initial stage. Erdas LPS.

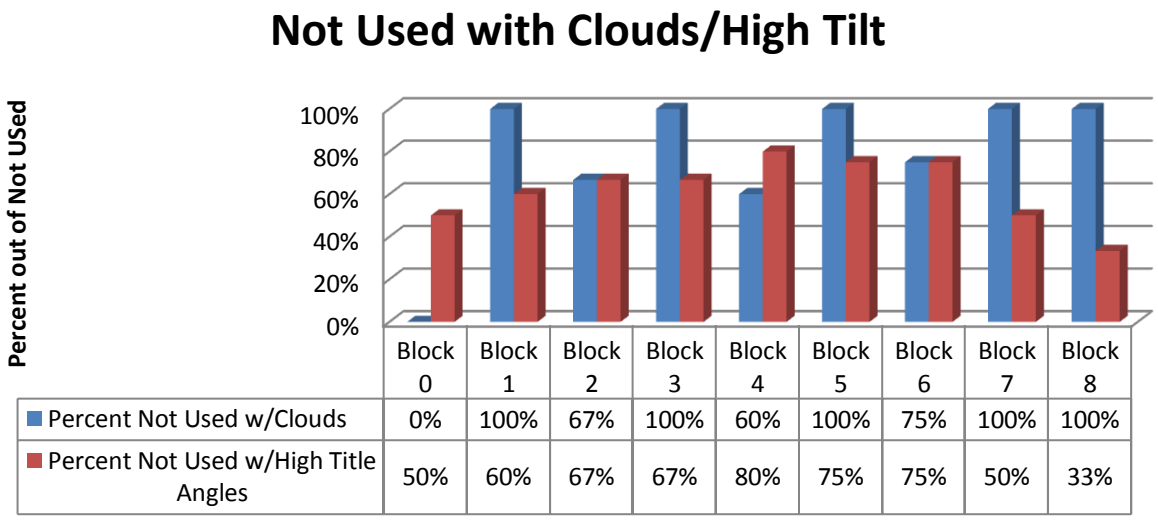

	Block 0	Block 1	Block 2	Block 3	Block 4	Block 5	Block 6	Block 7	Block 8
Percent Not Used w/Clouds	0%	100%	67%	100%	60%	100%	75%	100%	100%
Percent Not Used w/High Title Angles	50%	60%	67%	67%	80%	75%	75%	50%	33%

Figure 4-25. Cloud presence and high pitch-roll values impact on tie point search. Erdas LPS.

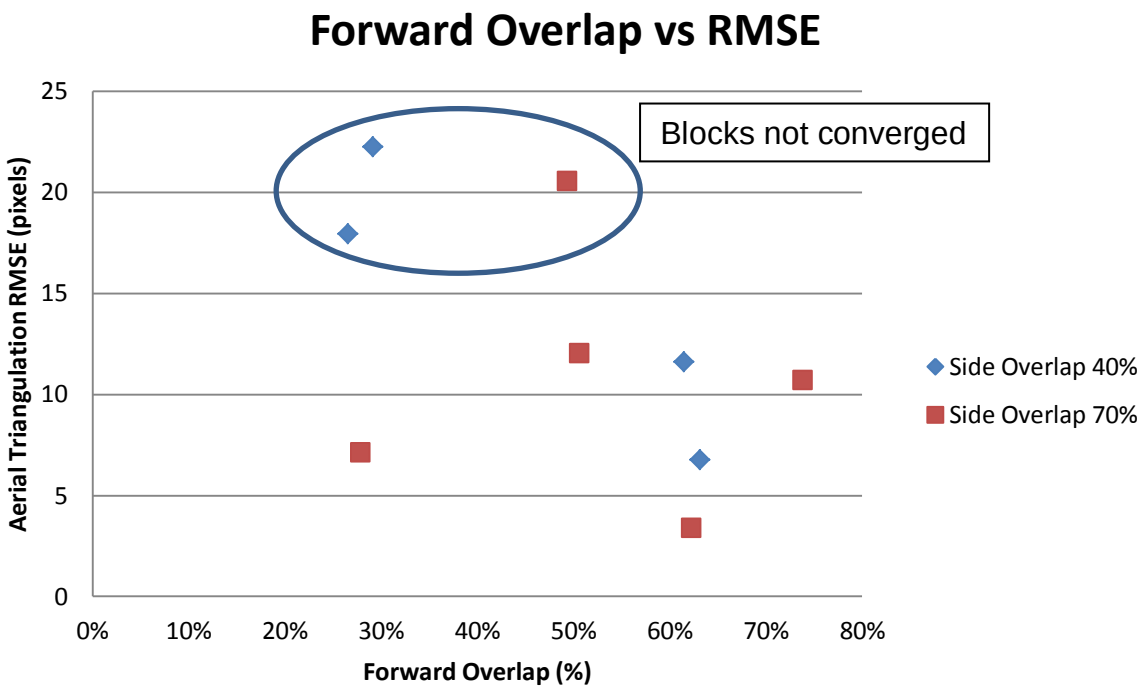

Figure 4-26. Relation between overlap percentages and Root Mean Square Error (RMSE) in aerotriangulation. Erdas LPS.

CHAPTER 5
CONCLUSIONS

Comparison

2d3 Altimap created visually pleasant mosaics in all configurations done with smooth seam-lines, great for GIS and Remote Sensing image processing applications. The mosaicking in the trees were good also with minimum errors. The errors found in these mosaics were located in the edges of the area of study, where no overlap occurred. 2d3 Altimap also applied auto level corrections and color balancing to the images, correcting shadow effect by clouds. Figure 5-1 shows a mosaic created by 2d3 Altimap and the zoom to one matching error, where the street was discontinued.

EnsoMOSAIC created visually pleasant mosaics as well. The histogram matching between images created the smoother seam-lines in the mosaics by EnsoMOSAIC. These outputs looked pretty similar to the final result of 2d3 Altimap. These resulting mosaics can be used for GIS and Remote Sensing image processing applications. Sun corrections can be done automatically by the software if UTC date and time where inputted on the first step of the post-processing. Figure 5-2 shows the resulting mosaic with the histogram matching and bilinear interpolation resampling options.

Erdas LPS created the least pleasant mosaics of the three software programs evaluated, there was not a proper automatic seam-line creation, and no sun correction or color balancing where applied, for this the image has to go through more radiometric manipulation. A mosaic created by LPS is shown by Figure 5-3.

EnsoMOSAIC was capable than Erdas LPS in finding more automatic tie points on the first interaction of ATP process done with similar options for both software, as shown in Figure 5-4. This is true for every block configuration used. Figure 5-5 shows

that even though EnsoMOSAIC found more points also in general LPS had more tie point found accuracy with more of the blocks assessed had more than 60% of tie points right up to 90%.

Despite the fact that LPS had more tie points accuracy, the algorithm used by EnsoMOSAIC results with less Root Mean Square Error (RMSE). Figure 5-6 shows the comparison in RMSE(Pixels) between both software.

2d3 Altimap can process mosaics within hours of data acquisition while the two other software can take more than five days, working 8-plus hours per day, for standard missions of 300 to 400 images.

Conclusions

2d3 Altimap is a good 2D georeferenced mosaic solution for UAS imagery, not as its price suggests (US$150.00). The mosaics created by Altimap are very well georeferenced, even if it does not contemplate exterior orientation parameters (pitch, roll and yaw angles). Between the packages that use exterior orientation parameter, the better equipped for UAS imagery mosaicking is EnsoMOSAIC resulting in better resampled ortho-mosaics and lower RMSE adjustments. The DEM generated by both EnsoMOSAIC and LPS were not very reliable, compared to existing DEM.

My recommendations are that UFUASRG and ACOE buy 2d3 Altimap solution for fast mosaic applications with good accuracy. I also recommend to use EnsoMOSAIC for missions using GCPs for better accuracies, and for flights with high winds that make the aircraft flights rougher.

Also, for better mosaics a camera calibration protocol has to be created for the current payload, where the calibration procedure would be done periodically, every certain amount of flights. Further a payload with a better camera would help in the

processing, like an industrial digital camera that the UFUASRG is trying to implement. For better positional accuracies, and perhaps better image matching in processing, a payload with differential or RTK GPS aboard would improve these positional accuracy of the system.

The three software assessed were able to process at less than standard overlap percentages (60% forward, 35% side), but the flight planning has to be designed for at least these values for better processing.

Recommendations

In future research about this subject, a positional assessment of the software has to be done. High resolution aerial or satellite images updated to any particular mission to be done are rare, for this kind of project concrete plates, monuments or markings like the ones used for GCPs have to be included in the area of study. This control points have to be measured with high accuracy surveying techniques, like RTK GPS, to achieve accurate coordinates, and this coordinates to be assessed with the final mosaics of the different software.

Using high accuracy surveying techniques a DEM have to be created and be compared with the DEM created by the software pixel by pixel to achieve a good elevation measurement capability assessment of the software.

Also, the results should be compared using calibrated camera parameters and without them, in order to get the impact of camera calibration procedures in post-processing for UAS photogrammetry.

Figure 5-1. Resulting mosaic using 2d3 Altimap. (Left) Mosaic of Block 0 done with 2d3 Altimap (Right) zoom to west zone of mosaic showing smoothness of seam lines and matching errors.

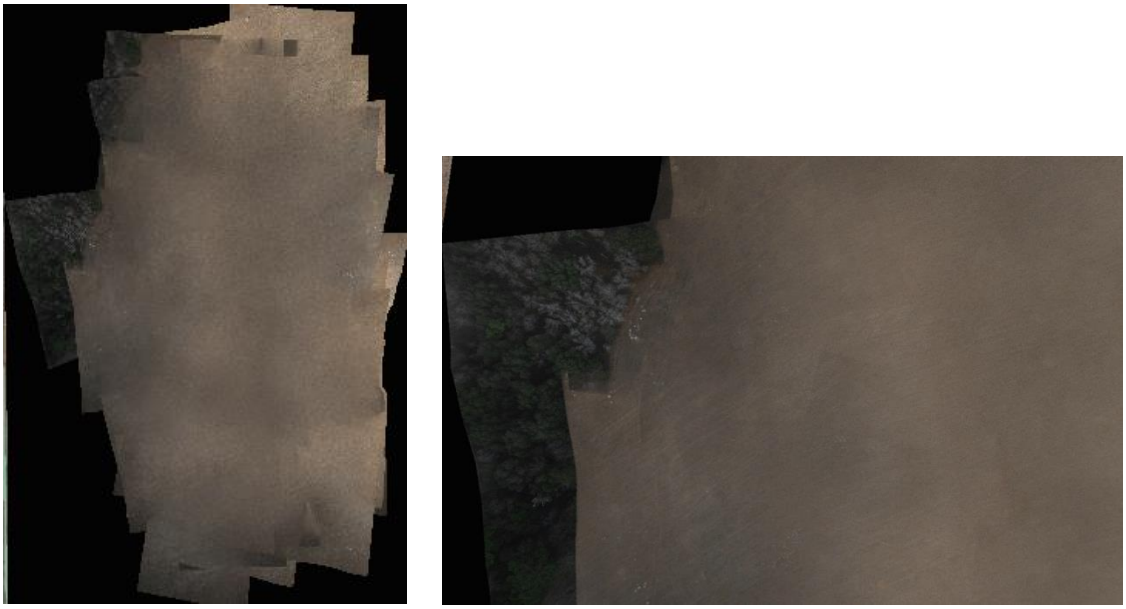

Figure 5-2. Resulting mosaic using EnsoMOSAIC. (Left) Mosaic of Block 0 done with EnsoMOSAIC (Right) zoom to west zone of mosaic showing smoothness of seam lines (histogram matching option).

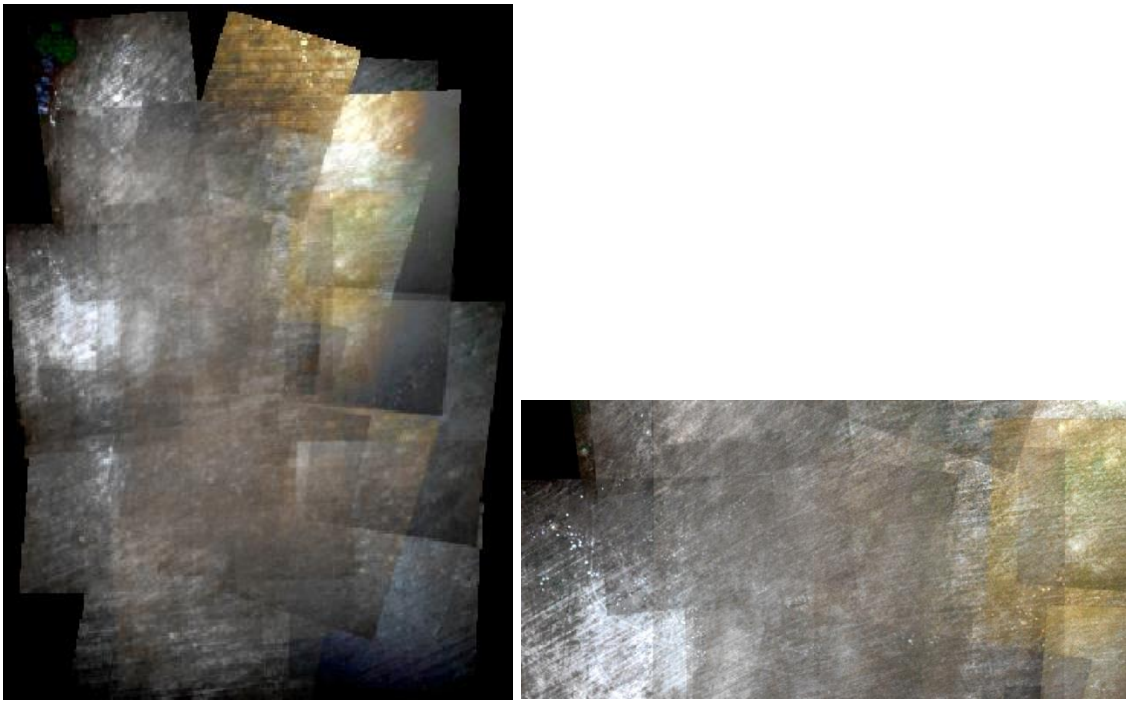

Figure 5-3. Resulting mosaic using Erdas LPS. (Left) Mosaic of Block 6 done with Erdas LPS (Right) zoom to west zone of mosaic showing smoothness of seam lines (average option).

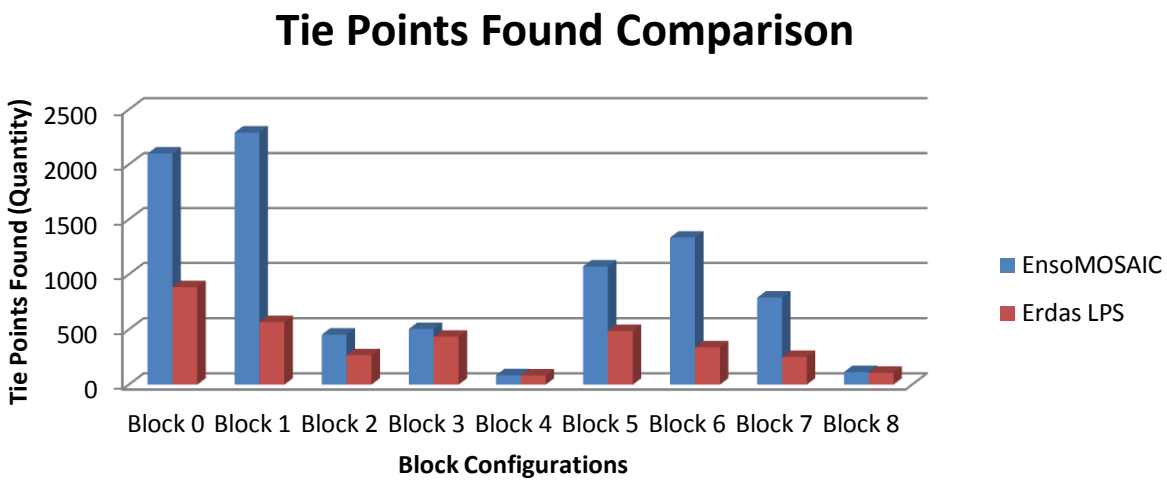

Figure 5-4. Comparison between EnsoMOSAIC and Erdas LPS in automatic tie point found.

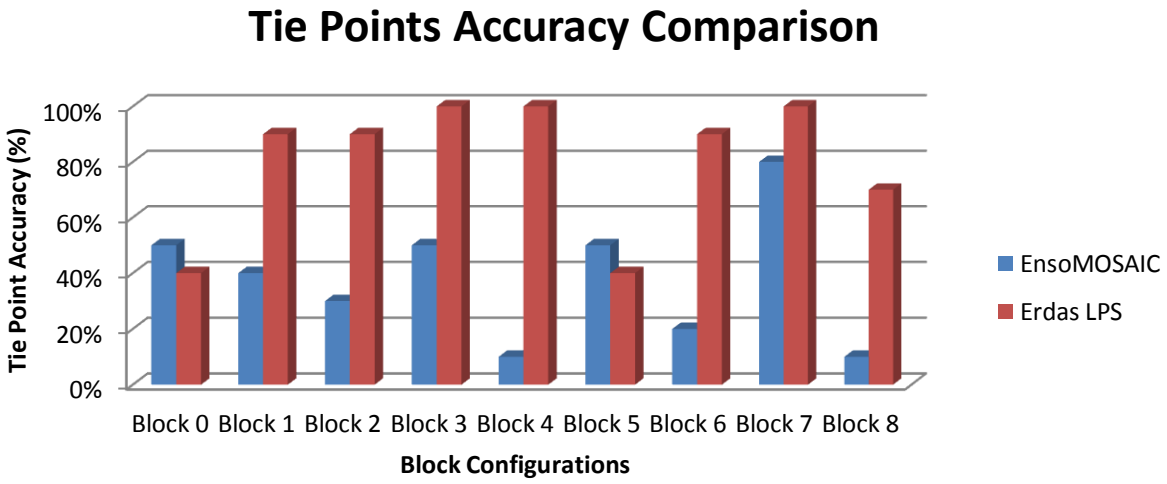

Figure 5-5. Comparison between EnsoMOSAIC and Erdas LPS in automatic tie point accuracy.

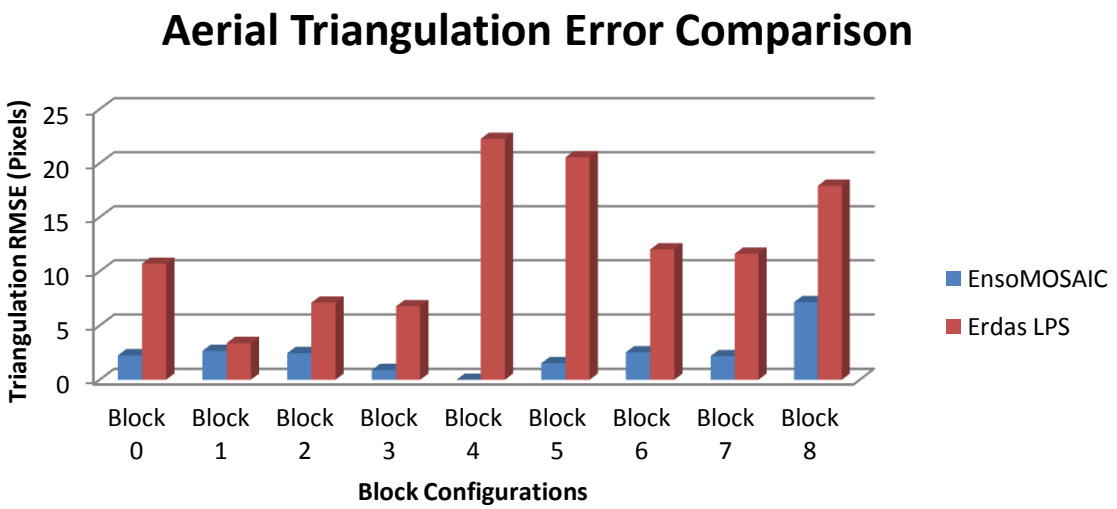

Figure 5-6. Comparison between EnsoMOSAIC and Erdas LPS in aerial triangulation error.

APPENDIX
IMAGE EXIF DATA READERS

For the 2d3 Altimap, one important part of the processing steps is to write the EXIF data to the collected imagery from the UAV. There are great online tools that can be used to verify the data is written correctly to the images. The following are two of the tools that give more information, including geotags of the image, camera info, and other parameters on the moment of the capture: http://regex.info/exif.cgi/exif.cgi and http://www.exifdata.com . (See Figures A-1 and A-2 for screen captures of examples of both pages).

Figure A-1. Jeffrey´s Exif Viewer, showing the location of an Archer Field Mission Image using the EXIF info written to it. Source (http://regex.info/exif.cgi/exif.cgi).

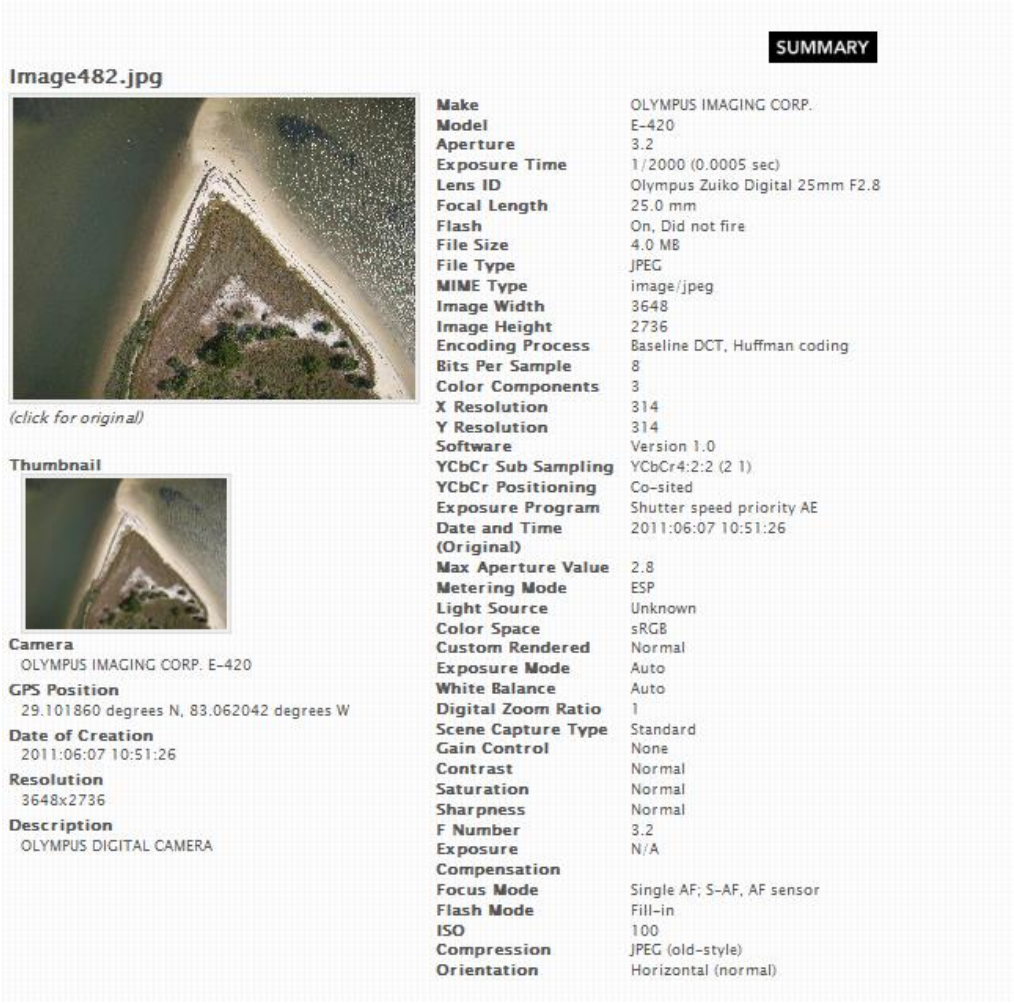

Figure A-2. Example of all the data contained in EXIF format written in an image. Source: (www.exifdata.com).

LIST OF REFERENCES

Aber, J.S., I. Marzolff and J.B. Ries, 2010. *Small-Format Aerial Photography, Principles, Techniques and Geoscience Applications*, First Edition, Elsevier, Amsterdam, The Netherlands, 266 p.

Ackermann, F., 1983. *High precision digital image correlation* Paper presented at 39th Photogrammetric Week, Institute of Photogrammetry, University of Stuttgart, pp. 231-243.

Afek, Y. and A. Brand, 1998. Mosaicking of Orthorectified Aerial Images, *Photogrammetric Engineering & Remote Sensing*, 64 (2): 115-125.

American Society of Photogrammetry,1980. *Photogrammetric Engineering and Remote Sensing,* 46 (10): 1249.

Burgess, M.A., P.G. Ifju, H.F. Percival, J.H. Perry, and S.E. Smith, 2009. *Development of a survey-grade sUAS for natural resource assessment and monitoring*, Slide presentation, Florida Cooperative Fish and Wildlife Research Unit Annual Coordinating Committee Meeting, Gainesville, FL. 32611.

Buyuksalih, G. and Z. Li, 2003. Practical Experiences with Automatic Aerial Triangulation Using Different Software Packages, *Photogrammetric Record*, 18 (102): 131-155.

Campbell, J.B., 2011 *Introduction to Remote Sensing*, Fifth Edition, Guilford Press, New York, 684 p.

Digicamhelp. “What is ISO?” Digital camera help for beginners and beyond, Digicam Website. URL: *http://www.digicamhelp.com/camera-features/advanced-settings/iso/* (last date accessed: 18 July 2012).

Eisenbeiss, H., 2009. *UAV Photogrammetry*, Doctorate Dissertation, Institute of Geodesy and Photogrammetry, ETH Zurich. Zurich, 203 p.

Erdas Inc., 2010. *LPS Project Manager User´s Guide*, United States of America, 421 p.

Everaerts, J., 2008. The Use of Unmanned Aerial Vehicles (UAVS) For Remote Sensing and Mapping. *The International Archives of the Photogrammetry, Remote Sensing and Spatial Information Sciences*. XXXVII (B1): 1187-1191

Exif Data Viewer. “What is EXIF Data?” EXIFDATA Website, URL: *http://www.Exifdata.com* (last accessed: 25 July 2012).

Förstner, W., and E. Gülch, 1987. *A fast operator for detection and precise location of distinct points, corners and centers of circular features*, Paper presented at the Intercommission Conference on Fast Processing of Photogrammetric Data, Interlaken, Switzerland, pp. 281-305.

Ghosh, S.K., 2005. *Fundamentals of Computational Photogrammetry*, Concept Publishing Company, New Delhi, India, 254 p.

Granshaw, S. I., 1980. Bundle Adjustment Methods In Engineering Photogrammetry. *The Photogrammetric Record*, 10 (56): 181–207.

Grün, A. and E. P. Baltsavias, 1988. Geometrically constrained multiphoto matching, *Photogrammetric Engineering and Remote Sensing* 54 (5): 633-641.

Haarbrink, R.B. and E. Koers, 2006. Helicopter UAV for Photogrammetry and Rapid Response. *The International Archives of Photogrammetry, Remote Sensing and Spatial Information Sciences*, Antwerp, Belgium, XXXVI(1-W44): 4 p.

Heipke, C., 1997. Automation of interior, relative, and absolute orientation, *ISPRS Journal of Photogrammetry and Remote Sensing*, 52(1): 1-19.

Helava, U. V., 1988. Object space least square correlation, *International Archives of Photogrammetry and Remote Sensing,* 27 (B3): 321-331.

Herwitz, S.R., L.F. Johnson, S.E. Dunagan, R.G. Higgins, D.V. Sullivan, J. Zheng, B.M. Lobitz, J.G. Leung, B.A. Gallmeyer, M. Aoyagi, R.E. Slye and J.A. Brass, 2004. Imaging from an unmanned aerial vehicle: agricultural surveillance and decision support. *Computers and Electronics in Agriculture* 44 (1): 49-61.

Ionescu, D., 2010. Geolocation 101: How It Works, The Apps, and Your Privacy, PCWorld, URL: *http://www.pcworld.com/article/192803/geolocation_101_how_it_works_the_apps_and_your_privacy.html* (last accessed: 23 July 2012)

Jeffrey´s EXIF. Jeffrey´s EXIF Viewer, URL: *http://regex.info/exif.cgi/exif.cgi* (last accessed 13 October 2012).

Kasser, M. and Y Egels, 2002. *Digital Photogrammetry*, First Edition, Taylor & Francis, New York, 351 p.

Kennedy, R. and W.Cohen, 2003. Automated designation of tie-points for image-to-image coregistration, *International Journal of Remote Sensing*, 24(17): 3467-3490.

Konecny, G., 1994. *New Trends in Technology, and their Application: Photogrammetry and Remote Sensing—From Analog to Digital*. Thirteenth United Nations Regional Cartographic Conference for Asia and the Pacific, Beijing, China, 6 p.

Krzystek, P., T. Heuchel, U. Hirt and F. Petran, 1996. An Integral Approach to Automatic Aerial Triangulation and Automatic DEM Generation, *International Archives of Photogrammetry and Remote Sensing*, 31 (B3): 405-414.

Laliberte, Andrea, 2012. Mapping Rangelands With Unmanned Aircraft, Aerial Mapping Spring 2012, Professional Surveyor Magazine, URL: *http://www.profsurv.com/magazine/article.aspx?i=71086* (last accessed: 23 October 2012).

Lillesand, T., R. Kiefer and J. Chipman, 2008. *Remote Sensing And Image Interpretation*. Sixth Edition. Wiley and Sons. Madison, Winsconsin, 763 p.

Liu, X., P. Chen, X. Tong, S. Liu, S. Liu, Z. Hong, L. Li and K. Luan, 2012. UAV-based low-altitude aerial photogrammetric application in mine areas measurement, *Earth Observation and Remote Sensing Applications (EORSA), 2012 Second International Workshop:* 240-242.

Matthews, N. A., T.A. Noble and B.H. Breithaupt, 2012. Dinosaur tracks to dam faces: A new method for collecting three-dimensional data, *Geological Society of America Abstracts* 36(5): 348 p.

Morgado, A., and I. Dowman, 1997. A procedure for automatic absolute orientation using aerial photographs and a map, *ISPRS Journal of Photogrammetry & Remote Sensing* 52(4): 169-182.

MosaicMill Oy, 2009. *EnsoMOSAIC Image Processing User´s Guide*, Finland, 106 p.

Norut (Northern Research Institute). UAV Applications, Nortu Website, URL: *http://uas.norut.no/UAV_Remote_Sensing/Applications.html* (last accessed: 14 October 2012).

Perry, J., 2009. *A Synthesized Directly Georeferenced Remote Sensing Technique for Small Unmanned Aerial Vehicles*, Masters Thesis, School of Forest Resources and Conservation, University of Florida, Gainesvile, Florida, 154 p.

Qingyuan, L., L. Wenyang, Z. Lei, W. Jingling and L. You, 2011. A New Approach to Fast Mosaic UAV Images, International Archives of the Photogrammetry XXXVIII (1/C22): 6 p.

Rango, A. A. Laliberte, C. Steele, J.E. Herrick, B. Bestelmeyer, T. Schmugge, A. Roanhorse and V. Jenkins, 2006. Using unmanned vehicles for rangelands: Current applications and future potentials. *Environmental Practice*, 8 (3): 159-169.

Réstas, A., 2006. The regulation Unmanned Aerial Vehicle of the Szendro Fire Department supporting fighting against forest fires, *Forest Ecology and Management*, 234S (S233): 234-240.

Sawhney, H.S. and R. Kumar, 1999. True multi-image alignment and its application to mosaicking and lens distortion correction, *Pattern Analysis and Machine Intelligence, IEEE Transactions*, 21 (3): 235-243.

Schenk, T., 1997. Towards automatic aerial triangulation*, ISPRS Journal of Photogrammetry & Remote Sensing*, 52 (3): 110-121.

Schenk, T., 2004. From point-based to feature-based aerialtriangulation, *ISPRS Journal of Photogrammetry and Remote Sensing*, 58 (5-6): 315-329.

Shragai, Z, S. Barnea and A. Even-Paz, 2012. *Novel Matching Method for Handling Non-Standard Imagery: Automatic Tie-point Extraction*. GIM International, USA, pp 31-35.

Tang, L. J. Braun and R. Debitsch, 1997. Automatic aerotriangulation — concept, realization and results, *ISPRS Journal of Photogrammetry and Remote Sensing*, 52 (3): 122-131.

Turner, D. A. Lucier and C. Watson, 2012. An Automated Technique for Generating Geo-rectified Mosaics from Ultra-High Resolution Unmanned Aerial Vehicle (UAV) Imagery, Based on Structure from Motion (SfM) Point Clouds, *Remote Sensing Journal*, 4(5): 1392-1410.

Vosselman, G., and N. Haala, 1992. Recognition of topographic control points through relational mapping, *Journal of Photogrammetry and Remote Sensing* 60 (6): 170-176.

Vosselman, G., 1995. Applications of tree search methods in digital photogrammetry, *International Society of Photogrammetry and Remote Sensing (ISPRS) Journal of Photogrammetry and Remote Sensing,* 50 (4): 29-37.

Wang, Y., 1998. Principles and applications of structural image matching, *International Society of Photogrammetry and Remote Sensing (ISPRS) Journal of Photogrammetry and Remote Sensing* 53 (3): 154-165.

Watts, A., F. Percival, S. Bowman,D. Coffin,P. Ifju, A. Abd-Elrahman, B. Dewitt, Y. Kaddoura, A. Mohamed, J. Lane, K. Lee, L. Pearsltine, J. Perry and S.E. Smith,2010. *Scientific Applications of UAS: Biological Research and Natural Resource Monitoring*, University of Florida, Gainesville, FL. 32611.

Wilkinson, B.E., 2007. *The Design of Georeferencing Techniques for an Unmanned Autonomous Aerial Vehicle for Use with Wildlife Inventory Surveys: A Case Study of the National Bison Range, Montana*. Master's Thesis, School of Forest Resources and Conservation, University of Florida, 115 p.

Wolf, P.R. and B.A.Dewitt, 2010. *Elements of photogrammetry with applications in GIS*, Third Edition, McGraw Hill, Boston, Massachusetts, 608 p.

Zebedin, L., A. Klaus, B. Gruber-Geymayer and K. Karner, 2006. Towards 3D map generation from digital aerial images, *ISPRS Journal of Photogrammetry & Remote Sensing* 60 (6): 413–427.

BIOGRAPHICAL SKETCH

Héctor Yamil Rodríguez Asilis decided at a really young age that he was going to be a Civil Engineer, around ten years old, and everything that happened after that in middle and high school just confirmed his desire. His father is a Civil Engineer and Surveyor and his mother is a Civil Engineer as well, this made an environment for Yamil at very young ages around plans, maps and construction to a point that a client was at his dad office when he was 3 years old, and this baby boy entered the office took a project plan and explain what the legend meant on the plans, so starting at that age he knew at least how to read plans and maps. He is an avid golfer, playing almost to scratch golfer, and being on the Junior Dominican National Team twice and winning his Match Play Club Championship on his first try, and the younger one to date to accomplish it.

Yamil majored in Civil Engineering and was one of the few that graduated in the 4 years the program proposes, and with “Cum Laude” honors for having a GPA of 3.3 out of 4.0. One curious thing about Yamil, is that even though Civil Engineering has a relatively extensive field, he was always comfortable in every field he studied and worked, making this a tough decision on what area to make his specialization in graduate school. He co-opted for the biggest engineering company in the island, working as a field engineer. After graduation he went back to his beloved small town of Puerto Plata to work on the family owned engineering company with his parents, starting right out of the gate in the construction biggest commercial plaza ever on town as a field engineer, and working simultaneously on the geomatics division of the same company, where he later also did different certificates in boundary surveying and RTK GPS and Differential GPS Surveying, and after a good look at the market, and already

fascinated with the geomatics he decided to apply for graduate studies in the area of geomatics, ultimately deciding to go to University of Florida.

After a few semesters in the program he was hired on the UAV Project on the post-processing team, making this a great experience and helped him learn a lot about this new technology, the one that he will be venturing to take back to his home country as a business where he thinks there is a lot of applications with this in the DR. He is planning to graduate with a Masters of Science in Forest Resources and Conservation with a Concentration in Geomatics in December 2012. His time in Gainesville and University of Florida was great, he learned a lot of things, and met a lot of people who at the absence of his family, who were back in the DR, became his adoptive family in the good and the bad times. Go Florida Gators!!